Protein Denaturation at the Air–Water Interface in the Context of Nanoparticle Soft Corona Studies

*Mahima Unnikrishnan,[1] Martin Gruebele,[123] and Catherine J. Murphy[1]**

AUTHOR ADDRESS

[1]Department of Chemistry, University of Illinois Urbana-Champaign, Urbana, IL 61801, USA,

[2]Department of Physics, University of Illinois Urbana-Champaign, Urbana, IL 61801, USA,

[3]Center for Biophysics and Quantitative Biology, University of Illinois Urbana-Champaign, Urbana, IL 61801, USA

*to whom correspondence should be addressed: murphycj@illinois.edu

ABSTRACT

The interaction of proteins with surfaces can involve both protein binding and unfolding and has been investigated since the 1960s. Proteins in solution can adsorb onto and denature at both solid–liquid and gas–liquid interfaces, and the spontaneous adsorption of proteins on a nanoparticle (NP) surface to form a corona can be described as a specific case of adsorption at the solid-liquid interface, where the surface curvature also becomes important. While nanoparticles offer a large surface area, they are not the only surface in the sample that the proteins interact with due to the creation of other interfaces in an experimental setup. In this work, we examine the role of the air–water interface on protein denaturation in soft corona studies with citrate-capped gold nanoparticles. Chymotrypsin protein in the soft corona was observed to exhibit an inverse

relationship between concentration and denaturation, an air-water interface mediated trend which, without the right control experiments, can be misinterpreted to be caused by protein-NP interactions. We show that any protein denaturation observed comes from the synergistic effect of the air-water interface and agitation, and that NPs did not denature chymotrypsin in the "soft corona" in the absence of these two factors. While the propensity to adsorb and denature at hydrophobic interfaces varies among proteins with different structural properties, it is important to use simplified procedures that minimize interfacial areas other than the nanoparticle surface in corona studies to prevent misattribution of observed effects.

INTRODUCTION

The spontaneous adsorption of proteins onto a solid surface is a fundamental process that plays a key role in applications of nanomaterials in the biomedical field.[1,2] Interaction forces between the surface, the proteins, the solvent, small molecules, and any ions present in solution can guide the mechanism of adsorption and desorption of the protein to the surface. Protein-protein and protein-nanoparticle interaction forces can range from disulfide bridging, electrostatic interactions, and hydrogen bonds, to van der Waals interactions, and hydrophobic interactions.[3,4] The process of protein folding which results in the formation of a functional three-dimensional structure from polypeptide chains, involves formation of several weak interactions, and has been described as a diffusional search on a free energy surface. Energy barriers to protein folding can be on the order of thermal energy (k_BT).[5,6] In vitro folding experiments have indeed shown that many cytosolic globular proteins possess relatively low folding equilibrium constants — meaning they frequently

unfold and refold throughout their life cycle, with shifts in equilibrium driven by perturbations in solvation environment, for example — and this conformational flexibility is a characteristic that helps proteins carry out their function.[7,8] Kinetic and thermodynamic investigations have consistently suggested that substantial structural alterations can take place when a protein adsorbs onto a surface. This can lead to unwanted biological side effects, such as a loss of activity due to protein conformational changes. [9–15]

Protein binding to nanoparticle surfaces is often described as a "corona" on the surface, an equilibrium phenomenon regulated by on and off rate constants. Proteins binding with higher affinity, directly on the nanoparticle surface, and having longer residence time on it are considered to be the "hard" corona, and the less tightly bound proteins, interacting mostly by weak protein-protein interactions, with faster exchange rates in the corona are referred to as the "soft" corona.[16–19] A majority of experimental investigations on nanoparticle protein coronas focus on identifying the types and quantities of proteins comprising the corona through a multi-step process of separating NPs from biofluid. This involves incubating NPs with a biofluid such as blood serum or cell lysate for corona formation, then separating unbound proteins from the NPs, typically through techniques like centrifugation or magnetic retrieval followed by washing.[20] During this workflow, only proteins with strong binding affinity, characterized by low dissociation rates, will remain bound to the NPs during the separation step, while those with weak binding affinity are generally lost. Thus, studies on protein conformational changes upon adsorption to a NP surface in the literature primarily pertain to hard corona proteins. [21–23]Adsorption of proteins on the NP

surface and subsequent changes to their structure have been shown to depend on the proteins' native fold, stability, and isoelectric point,[24] as well as the NP surface charge and curvature.[25,26]

Due to their dynamic nature, soft corona proteins cannot be isolated in the same manner as the hard corona, and their behavior is typically studied using *in situ* methodologies.[18] Devineau and co-workers used cryo TEM and synchrotron-radiation circular dichroism techniques to demonstrate that hemoglobin has the capacity to develop either a hard or soft corona around silica NPs, contingent upon the pH conditions.[26] Another investigation utilizing *in situ* click chemistry also showed that the proteins in the hard and soft coronas could be the same species, coexisting spatially but varying in their residence time, influenced by factors such as their abundance, affinity for the NP surface, and local density. [27] Hence, the distinction between the hard and soft coronas do not represent two entirely separate layers of proteins formed through sequential deposition, as was initially believed; rather, the corona progresses from harder to softer with distance from the nanoparticle. *In situ* analysis of the corona on liposomes formed by incubation with plasma suggested that soft corona contributed to the stealth properties of the liposome, thus modulating its biological identity.[28] Weakly interacting proteins on silica and polystyrene NPs were also found to influence nanoparticle-cell association.[27]

A recent work published by Riley et al. discussed a rare case in the protein corona literature of *ex situ* soft corona protein conformation, where proteins recovered in the NP-free supernatant by centrifugation is referred to as the soft corona.[29] This work reported that commercially purchased bovine alpha chymotrypsin (ChT) formed weak interactions with citrate stabilized gold

nanoparticles (AuNPs), and when these "soft corona" proteins were separated from the NPs, they remained denatured. A low protein: NP ratio in solution and long incubation time lead to more protein denaturation. ChT has been in the past reported to denature in the hard corona of anionic AuNPs, [30] and the extent of denaturation was reported to increase with time of incubation of protein and NPs. If it is generally the case that proteins become denatured "permanently" after transiently binding to NPs, even when desorbed from the NP surface, then the implications for the use of NPs in biomedicine are vast and concerning: denaturation can cause familiar globular proteins to lose their function and perhaps aggregate into amyloid species.[31–34]

In most experimental setups, however, interfaces like an air-solvent interface (resulting from a tube with an airhead, bubble formation, etc.) and/or solid-solvent interface (in contact with container walls) exist where proteins can potentially adsorb and undergo conformational changes. Protein adsorption at interfaces is a well-known challenge in biopharmaceuticals, as therapeutic protein molecules may encounter a variety of interfaces during their manufacturing, transportation, and storage. Agitation-induced exposure to the air–water interface can lead to protein aggregation. [35–37] The mechanism of protein aggregation in this case can be explained using contraction-expansion cycles of the air-water interface as follows. [38] Agitation leads to cyclic changes in the air-water interfacial area—expansion promotes protein adsorption and enrichment at the interface, while contraction expels accumulated aggregates. This repeated regeneration of the interface during compression and dilation cycles causes progressive and cumulative protein damage. The aggregation of therapeutic antibodies at air–water interfaces has been investigated using techniques such as microbubble aeration and interfacial shear rheology. [39,40] To mitigate these

interfacial effects, antibody formulations often include additives like surfactants, which can help reduce protein aggregation.[41,42]

In nanoparticle-protein studies investigating protein structural changes induced by the NP, the role of other interfaces is rarely discussed. We hypothesize that this oversight could lead to erroneous conclusions about the impact of NPs on protein denaturation in the corona. In this work, we analyze soft corona proteins following their interaction with citrate-capped AuNPs using two model proteins—chymotrypsin and bovine serum albumin—and aim to distinguish the contributions of non-nanoparticle interfaces (air–solvent and container wall–solvent) from those of the nanoparticle–solvent interface in protein denaturation.

EXPERIMENTAL SECTION

Reagents

Tetrachloroauric (II) acid trihydrate ($HAuCl_4 \bullet 3H_2O$), hydroquinone, α-chymotrypsin from bovine pancrease, bovine serum albumin, sodium phosphate dibasic heptahydrate ($Na_2HPO_4 \bullet 7H_2O$), sodium phosphate monobasic monohydrate ($NaH_2PO_4 \bullet H_2O$), trisodium citrate dihydrate ($Na_3C_6H_5O_7 \bullet 2H_2O$) were purchased from Sigma-Aldrich. Low protein binding polypropylene tubes and low protein binding plastic pipette tips were purchased from Eppendorf. Teflon tubes were purchased from ThermoFisher Scientific.

Preparation of protein aliquots

The α-chymotrypsin stock (2000 μg/mL) and bovine serum albumin stock (3000 μg/mL) were prepared by dissolving as-purchased lyophilized powder in 10 mM sodium phosphate buffer (pH 7.5). The solution was syringe filtered using a 0.22-micron filter and aliquoted into 100-500 μL

volumes in 1.5 mL polypropylene microcentrifuge tubes. The aliquots were flash frozen using liquid nitrogen and stored at – 80 °C. [43,44] Aliquots were freshly thawed before using on the same day and did not undergo multiple freeze-thaw cycles. Protein solutions were characterized using MALDI mass spectrometry, circular dichroism, and fluorescence spectroscopy. Each new batch of ChT protein purchased from Sigma-Aldrich was characterized before use. BSA from a single bottle purchased from Sigma-Aldrich was used for all experiments.

Synthesis and characterization of 60-nm and 40-nm citrate-stabilized AuNPs

Citrate-capped AuNPs were synthesized using a previously reported method. [45] Gold seeds were synthesized by bringing a mixture of 500 µL of 1% w/v $HAuCl_4 \bullet 3H_2O$ and 50 mL of Nanopure H_2O to a boil while stirring, followed by addition of 1500 µL of trisodium citrate dihydrate (1% w/v). The solution was removed from the heat and stir plate after ~ 10 minutes when the color of solution changed from golden to red. The seeds were then used to prepare the growth solution for 60-nm spheres. In a 500 mL Erlenmeyer flask, 4.5 mL of gold seeds was introduced to a stirring mixture of 2.5 mL of $HAuCl_4 \bullet 3H_2O$ (1% w/v) and 240 mL of Nanopure H_2O at room temperature. Then, 550 µL of trisodium citrate dihydrate (1% w/v) and 2.5 mL of hydroquinone (0.03 M) were added to the solution one after the other quickly. The solution was allowed to stir for 1 hour before centrifugation to purify (600*g* for 30 mins) and was then resuspended in water. To synthesize the 40-nm spheres, a similar procedure was followed and ratio of ingredients in the growth solution changed to increase the volume of seeds added. 10 mL of seed solution were added to a mixture of 234.45 mL of H_2O and 2.5 mL of $HAuCl_4 \bullet 3H_2O$ (1% w/v). Then 550 µL of trisodium citrate dihydrate (1% w/v) and 2.5 mL of hydroquinone (0.03 M) were quickly pipetted into the solution.

The solution was allowed to stir for 1 hour before centrifugation to purify (7000*g* for 20 mins). The concentrated NP pellet was then resuspended in water. Extinction spectra was collected using an Agilent Technology Cary 5000 UV-vis-NIR spectrometer to determine concentration of particles in the stock solution. Hydrodynamic light scattering and ζ-potential of the NPs were measured using a Malvern Zetasizer Nano ZS. Transmission electron microscopy (TEM) micrographs of the NPs in water were obtained by drop-casting onto a copper grid with carbon type-B 300 mesh (01813-F, Ted Pella) before imaging on JEOL 2100 TEM operated at 200 keV.

Dynamic light scattering (DLS) titrations of protein with AuNPs

Titration curve samples were prepared in 10 mM sodium phosphate buffer, pH 7.5 for ChT and in Nanopure H_2O, pH 6.0 for BSA. Each titration point sample was prepared in a separate microcentrifuge tube. 4 measurements per sample were taken after 1 hour of incubation (still sample) at room temperature on a Malvern Zetasizer Nano ZS instrument in disposable cuvettes.

Incubation of NP and protein for soft corona studies

After a 1.1 mL protein+NP solution was incubated for 24 h in a 1.5 mL volume tube (low protein binding microcentrifuge tube), the solutions were centrifuged at 13000*g* for 10 mins and the top 900 μL of supernatant was retrieved to collect "soft corona" sample. Protein + NP samples in a low protein binding polypropylene tube were laid sideways to agitate gently on an orbital shaker set to 100 rpm unless otherwise noted. Since we pulled down all NPs using centrifugation, the AuNPs should cause no interference with the fluorescence or circular dichroism (CD) spectra of the supernatant.

Circular dichroism and fluorescence spectroscopy of proteins

Fluorescence measurements were conducted on an FP8300 spectrofluorometer equipped with Peltier temperature control S-2 (JASCO) and QuantaMaster 400 scanning spectrofluorometer. Tryptophan and tyrosine residues were excited at 280 nm, and emission spectra were collected from 290 to 450 nm. Spectra were measured in 200 μL quartz cuvettes. Circular dichroism was measured using a J-715 spectropolarimeter with Peltier temperature control (JASCO). Unless otherwise noted, all spectra were recorded from 260 to 190 nm averaging over ten accumulations in a 1 or 2 mm pathlength quartz cuvette. Thermal melts were done using a 2 mm path length cuvette. CD spectra of samples at protein concentrations ≤ 20 μg/mL were measured on a Jasco J-1500 spectrophotometer using a 1 cm pathlength quartz cuvette. Cuvettes were cleaned with milliQ water or dilute soap solution between samples. The photomultiplier voltage was maintained between 300-700 V for measurements. Secondary structure estimation from spectra was conducted using BeStSel software after baseline subtraction.[46]

Bicinchoninic Acid (BCA) assay for protein quantification

A set of protein + NP samples at the same concentrations used for the DLS titrations was prepared, along with control samples that had the same concentration of protein but no NPs in them. All samples were incubated at room temperature for 24 h. Both set of samples were centrifuged at 13000*g* for 5 mins and the NP-free supernatant was used for the BCA assay. The concentration of protein added was calculated as the difference of protein in a solution without NPs and the protein left in the supernatant after centrifugation in the samples containing NPs. A SpectraMax M2 plate reader (Molecular Devices) was used to read absorbance at 562 nm of 96-well plates. Low protein binding plastic tubes and pipette tips were used during the experiment.

RESULTS AND DISCUSSION

Circular dichroism and intrinsic fluorescence measurements of chymotrypsin

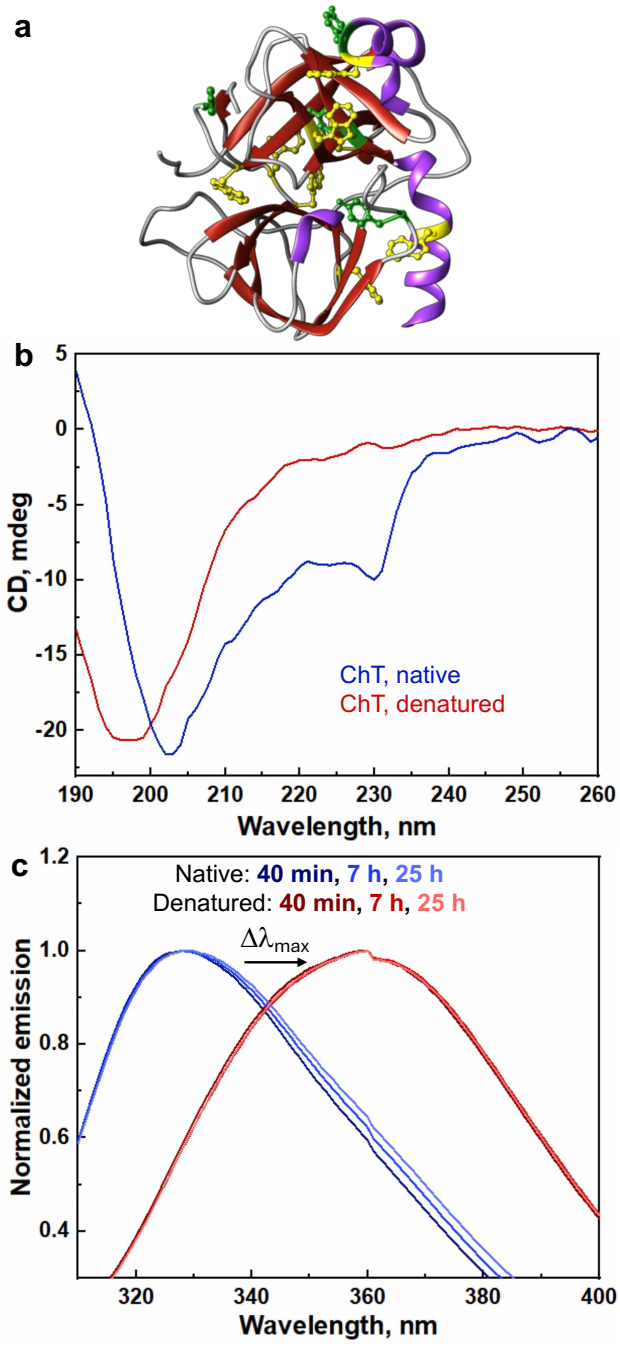

Figure 1. ChT protein structure, CD and fluorescence spectra. (a) Structure of alpha-chymotrypsin (PDB file 3BG4) rendered using Chimera. Helices are shown in purple, strands in red and coils in gray. Tryptophan residues are shown in yellow, and tyrosine residues in green. (b) CD spectra of native (blue) and thermally denatured (red) ChT. Denatured ChT was incubated in

a 60 °C water bath for 1 h. Spectrum of native ChT has been normalized to data point at 220 nm of denatured ChT spectrum. (c) Normalized emission from protein excited at 280 nm before (blue) and after (red) thermal denaturation. Time points in (c) denote time of incubation at RT post incubation in hot water bath for denaturation. Samples were cooled down to 20 °C for spectral measurement.

Chymotrypsin has 8 tryptophan residues and 4 tyrosine residues in the monomer protein (**Fig. 1a**). The protein has 245 amino acids with a mass of 25.7 kDa, and a net positive charge at pH 7.4. Reported hydrodynamic radius of a 0.5 mg/mL ChT solution is 2.27 nm.[47] Due to the presence of multiple aromatic amino acid residues, the protein has a strong absorbance peak at 280 nm and the intrinsic Trp/Tyr fluorescence can be monitored to analyze changes in structure of the protein as the emission intensity and wavelength (change in quantum yield and fluorescence lifetime) is very sensitive to the microenvironment of the residues.[48,49] Changes in the secondary structure of the protein can be monitored using circular dichroism.

Heating is one of the easiest methods to denature a protein without introducing a new denaturant molecule into solution that can potentially interfere with different analytical techniques used to characterize protein-NP interaction as well as subsequent denaturation of the protein. We heated the protein solution at 60 °C for 1 h and found that ChT can be irreversibly denatured at this condition (**Fig. 1**). Upon thermal denaturation, the CD spectrum of ChT protein shows significant differences; the peak at 230 nm disappears, and the peak around 205 nm blue shifts. The spectrum of denatured protein looks similar to that of a random coil CD spectrum (**Fig. 1b, S1a**). When the intrinsic tryptophan fluorescence emission of chymotrypsin is measured as temperature is varied from 10 to 95 °C, there is a decrease in emission intensity and a red shift of ~ 30 nm in the peak maximum wavelength when excited at 280 nm, moving from 328 nm at low temperature to 360

nm at high temperature (**Fig. 1c, S1b**). A red shift and decrease in intensity correspond to the aromatic residues (primarily Trp) being in a more polar environment as the protein unfolds and the buried residues are exposed to the aqueous solvent.[50,51]

Chymotrypsin denaturation in the soft corona of citrate-capped AuNPs

Soft corona studies were performed using 0.025 nM 60-nm (diameter) citrate-capped AuNPs synthesized as described in the *Experimental Section* (see **Fig. S2** for TEM images of the NPs). ChT protein was added at increasing amounts to the as-synthesized AuNPs to obtain a DLS titration curve. NPs alone in sodium phosphate buffer were colloidally stable and showed no visible aggregation. The DLS titration showed apparent protein saturation at dilute concentrations of ChT as shown in **Fig. 2a**. The hydrodynamic nanoparticle diameter increased with the addition of protein initially and then leveled off around 20 μg/mL of ChT for 0.025 nM NPs. The Langmuir adsorption isotherm fit well to the DLS data (**Fig. 2a**) indicating that adsorbed protein may be forming a monolayer with a K_a for adsorption $(1.95 \pm 0.65) \times 10^7$ M^{-1} (error is the standard deviation from K_a of the 3 titration sets). The polydispersity index during DLS measurements remained low across the different samples, confirming that the increase in diameter does not come from nanoparticle aggregation.

We also monitored the adsorption of ChT to the NPs using UV-Vis spectroscopy. There is no new peak or increased scattering at the longer wavelengths in the extinction spectra which indicate absence of aggregation of NPs in solution (**Fig. 2b**). As the protein is titrated into a solution of 0.025 nM NPs in buffer, the localized surface plasmon resonance (LSPR) peak of the AuNPs show

a slight red shift of 3 nm (**Fig. 2c**). The adsorption of protein on the NP surface changes the local refractive index which leads to this red shift in the LSPR peak.[52,53]

To determine whether the proteins do indeed form a hard corona on the NP surface, DLS samples were centrifuged to pull down all the nanoparticles and the proteins that are tightly bound to the surface. The clear supernatant was removed to get rid of any loosely bound excess protein in solution, and the pellet redispersed in a volume of buffer equal to what was removed. After the first wash, the hydrodynamic diameter for the samples at higher protein concentrations did not significantly change (**Fig. S3a**). This result indicated that the proteins likely form a strongly-bound layer (hard corona) on the NP surface. Next, we determined the actual concentration of ChT protein bound to the NP surface using a BCA assay in a 96-well plate (see *Experimental Section* for details). We prepared a standard curve for absorbance values using known concentrations of chymotrypsin (**Fig. S3b**), to measure the unknown concentration of chymotrypsin adsorbed on the NPs. The average protein concentration bound to 0.025 nM NPs was 3.4 $\pm$ 0.6 μg/mL. This corresponds to an average of 5280 $\pm$ 932 proteins/NP. It is plausible that the pull-down process of NP+hard corona could trap some of the free proteins from solution in the pellet during centrifugation, so the proteins/NP number could be overestimated.

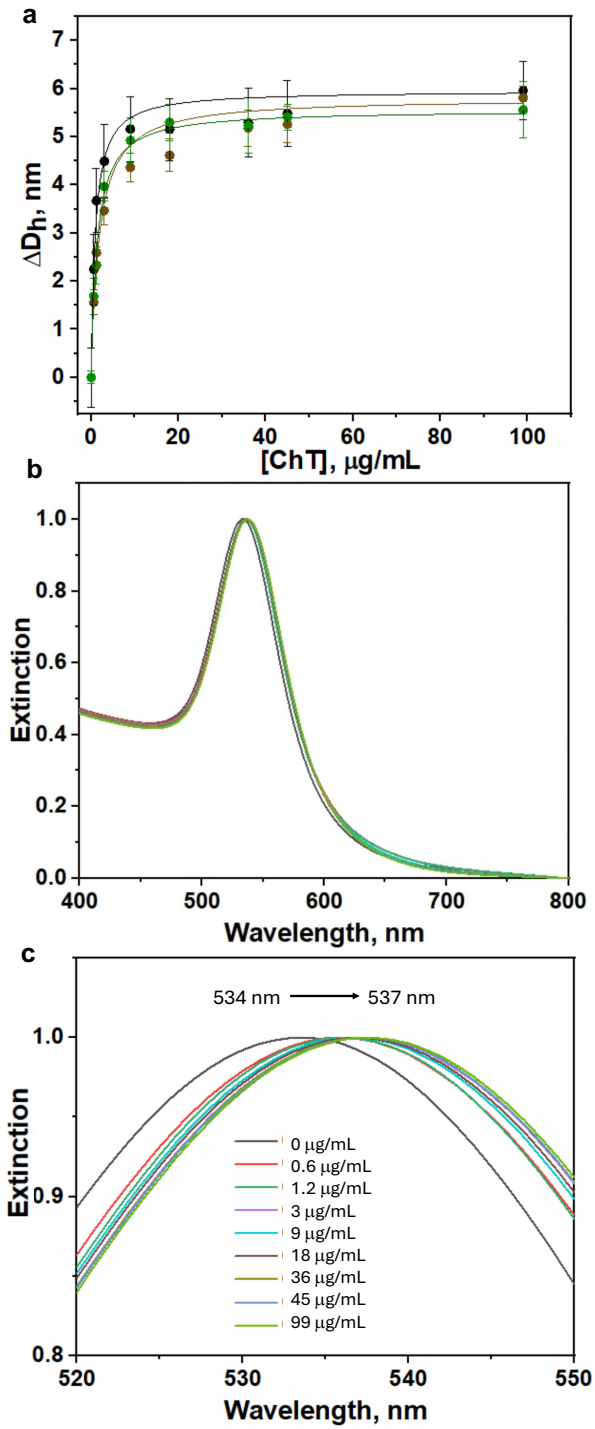

Figure 2. ChT corona formation on 60-nm AuNPs. (a) DLS titration curves from incubating increasing amounts of protein with 0.025 nM NPs in 10 mM sodium phosphate buffer at pH 7.5. Titration was performed thrice, and error bar on each point is the standard deviation from triplicate measurement of a sample. DLS data was fitted using the equation $\Delta D/\Delta D_{max} = K_a \times [protein]/ 1 + K_a \times [protein]$, $R^2 = 0.97$- 0.99 between the three replicates. (b) UV-Vis spectra of the NP+protein

samples used in (a). (c) Zoomed in image of the UV-Vis spectra in (b) showing the red shift in LSPR peak of the NPs as proteins coat the NP surface at increasing concentrations.

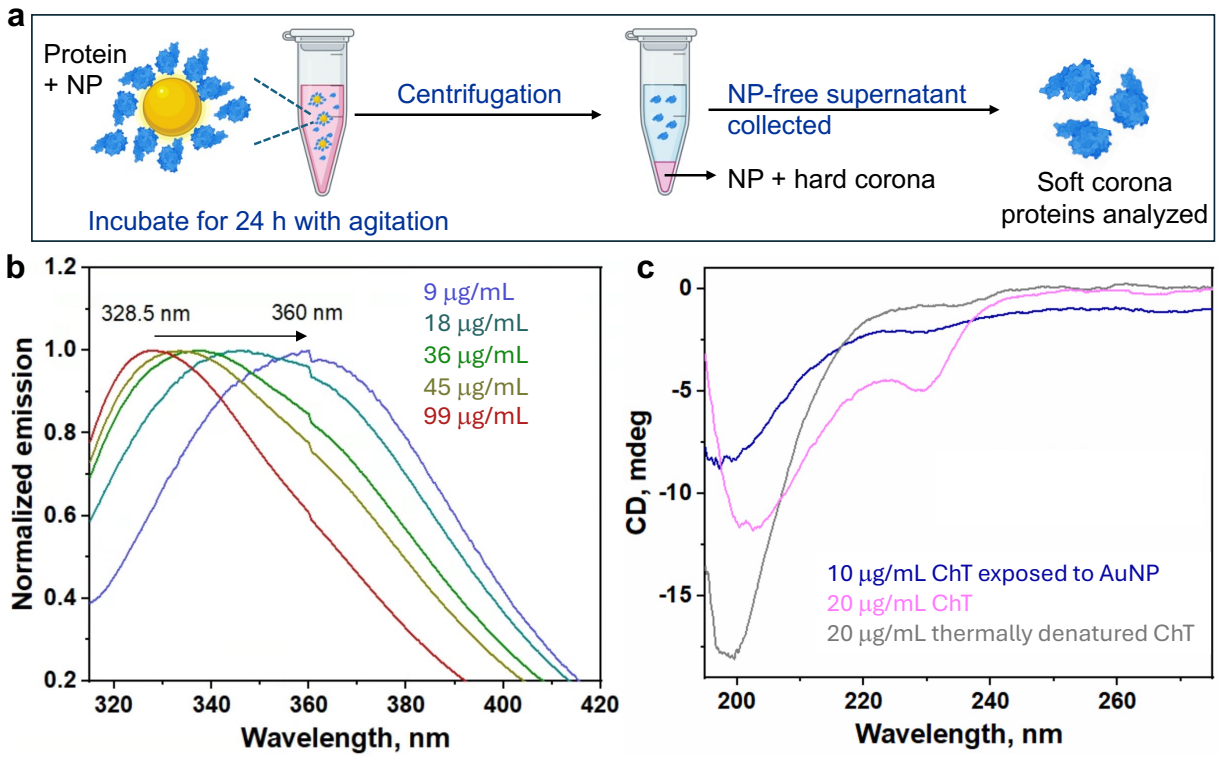

Figure 3. Soft corona studies of ChT + 60-nm AuNPs. (a) Schematic representation of experimental flow for soft corona studies. (b) Normalized Trp/Tyr emission spectra collected from NP-free supernatant after the indicated concentration of ChT was incubated with 0.025 nM 60-nm AuNPs for 24 h on orbital shaker (100 rpm) in a low protein binding plastic microcentrifuge tube. (c) CD spectra in 10 mM sodium phosphate buffer measured in 1 cm pathlength quartz cuvette. Baseline with buffer alone has been subtracted. Native ChT (pink) and thermally denatured ChT (grey) spectra are shown for reference. Illustration created with the help of BioRender. Unnikrishnan, M. (2025) https://BioRender.com/q59t118.

Thus, to generate a soft corona, protein +NP samples at ChT concentrations >3.4 µg/mL were left to gently shake at room temperature for a day followed by characterization of the supernatant (the easily removed "soft corona") using the workflow as depicted in **Fig. 3a**. We observed that there

is a significant red shift in the λ_{max} of protein emission (**Fig. 3b**) in the samples with lowest concentrations of ChT; this result implies that small amounts of protein remain denatured *after* exposure to the NPs. As the amount of excess ChT in solution increases beyond what is required for hard corona formation on the NPs, the peak of the emission spectra continues to blue-shift until the λ_{max} of emission matches that of free protein solution that has not been exposed to NPs. This result was also reported by Riley et al. in their study on 60-nm citrate-capped AuNPs and chymotrypsin, where the red shift in tryptophan emission was attributed to protein denaturation.[29] To further verify denaturation results, the CD spectrum of NP-exposed soft corona proteins (**Fig. 3c**) was collected after 24 h incubation with gentle shaking at room temperature. It is evident from the CD data that the spectrum for this sample is similar to that of denatured ChT (random coil-like).

To check if a NP with same surface chemistry, but smaller size (higher surface curvature) could yield similar effects in denaturing ChT, 40-nm citrate-capped AuNPs were synthesized (diameter = 39 $\pm$ 8 nm, see **Fig. S2c** for TEM) as described in the *Experimental Section*. DLS titrations were performed to infer ChT corona formation on these NPs (**Fig. S4a**), followed by measurement of fluorescence spectra of NP-free soft corona proteins using the same workflow as the 60-nm AuNPs. A red shift in the λ_{max} of protein emission was observed only in samples with lowest protein:NP ratio, and at higher ChT concentrations, the spectra matched with that of control samples kept still at RT for 24 h (**Fig. S4b**). Further, to verify whether the mechanism of ChT protein denaturation at low protein:NP ratios is from NPs actually denaturing proteins in the soft corona, or because NPs selectively adsorb a subpopulation of properly folded proteins in solution (assuming the stock solution has a small percentage of misfolded proteins in the mix to begin

with), we tested the binding affinity of chymotrypsin protein to AuNPs in the native versus denatured form. From DLS titration of thermally denatured chymotrypsin (ChT*) against 0.1 nM 40-nm AuNP (**Fig. S4c**), it was observed that although the maximum increase in hydrodynamic diameter is lower for ChT*, which can be rationalized due to change in orientation of protein adsorbed on NP surface before and after unfolding, K_a was on the same order of magnitude for native ($K_a = (2.25 \pm 0.25) \times 10^7$ M^{-1}) and denatured ($K_a = (1.25 \pm 0.25) \times 10^7$ M^{-1}) ChT.

Effect of incubation conditions on chymotrypsin denaturation

The time of incubation is an important factor in observing permanent protein denaturation as reported by Riley et al.,[29] and by Rotello and co-workers for hard corona denaturation of ChT by anionic AuNPs.[30] Hence, longer incubation times would be required to capture changes in protein conformation from transient interactions with the nanoparticles. We tested how the $\Delta\lambda_{max}$ of protein emission from the aromatic residues changes between a control and an NP- exposed chymotrypsin sample. Identical protein+NP samples was prepared by incubating 24 replicates of AuNPs with 10 μg/mL ChT (the concentration at which a significant red shift in protein emission post 24 h incubation was observed from prior experiments). At 1-hour intervals, one replicate was taken out of the shaker, and the tryptophan emission of soft corona proteins was measured by excitation at 280 nm, for 24 h. For each protein+NP sample prepared, a control sample which had only 10 μg/mL ChT and no NPs was processed the same way. From **Fig. 4a**, it is observed that the $\Delta\lambda_{max}$ of soft corona proteins increases with increasing incubation time for proteins exposed to the NPs (black points), but surprisingly, the control samples show a similar trend (green points). To cross-check the results from tryptophan emission, CD spectra of both NP-exposed soft corona proteins

and the control sample with only protein after 24 h incubation with gentle shaking at RT was collected. CD spectra for both samples after 24 h incubation resembled the spectrum of denatured ChT (**Fig. S4d**).

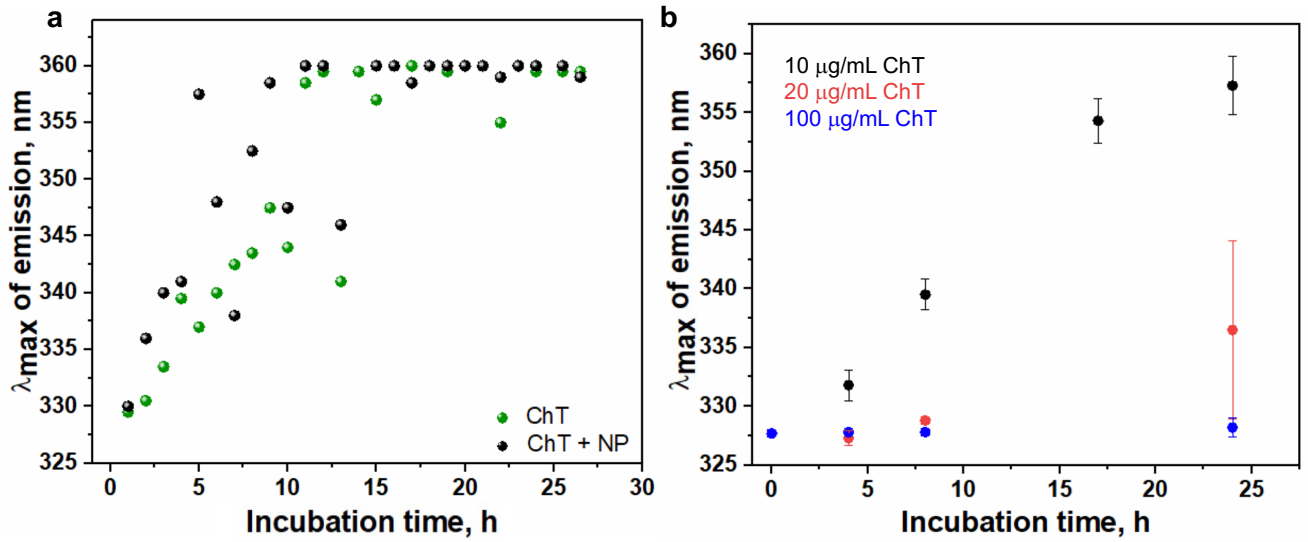

Figure 4. **Denaturation of ChT in samples without NPs.** (a) λ_{max} from Trp/Tyr emission of soft corona proteins exposed to NPs for different incubation times. In 'ChT+ NP' sample, 0.1 nM 40-nm citrate-capped AuNPs were incubated with 10 μg/mL ChT in a 1.5 mL microcentrifuge tube for different duration of incubation in buffer. The 'ChT' sample had only 10 μg/mL ChT in a microcentrifuge tube for the same duration of incubation. Total volume of solution was 500 μL. (b) Change in λ_{max} of emission from fluorescence spectra of ChT incubated at 3 different concentrations as a function of different incubation times. Error bars are standard deviations from three sample replicates per data point. Solution filled to 1 mL in a 1.5 mL volume low protein binding plastic microcentrifuge tube. All samples were in 10 mM sodium phosphate buffer, pH 7.5 and excited at 280 nm. All incubation was done at RT on an orbital shaker set to 100 rpm.

Why do proteins in control samples (without NPs) denature, on their own, with increasing incubation time? We systematically tested the effect of (a) temperature of incubation, (b) agitation conditions during incubation, (c) material of incubation vessel, and (d) concentration of protein in microcentrifuge tube during incubation. First, proteins were incubated at 3 different temperatures

(20°C, 25°C and 28°C), at different of agitation speeds on a shaker during incubation steps (0, 100 and 200 rpm). ChT at 10, 20 and 50 μg/mL ChT protein concentrations made up to 1 mL sample volume were incubated for 24 h in polypropylene microcentrifuge tubes, followed by centrifugation at 13000*g* for 5 mins, and then emission was measured. A red shift in λ_{max} was used to determine if the protein has been denatured and to what extent denaturation has occurred. The key takeaways from these experiments using ChT protein can be summarized as follows: (i) proteins did not denature significantly at any of the tested temperatures if they were incubated without shaking, (ii) protein denatured even at the lowest used temperature of 20°C if it was agitated vigorously (200 rpm) during the incubation step, although gentler shaking at 100 rpm also caused protein denaturation, (iii) at conditions where protein denaturation is observed, the effect is less significant when protein concentration is increased to 50 μg/mL (**Fig. S5**).

There is an observed difference in extent of protein denaturation at low versus high concentrations, which indicates there might be a surface effect at play here in addition to the effect of agitation. Bulk mediated denaturation should be higher at higher protein concentrations as rate of protein unfolding can increase with concentration due to protein-protein interactions.[36]Apart from the solid-liquid interface at the surface of the NPs in aqueous buffer, there is also the solid-liquid interface at the walls of the container and an air-liquid interface because the sample vial has not been filled all the way to the top during incubation. Proteins can adsorb at these interfaces [3,54,55] in addition to adsorbing on the NP surfaces, contribution from which we next investigated. Low protein binding plastic microcentrifuge tubes were used for these experiments (polypropylene), thus the walls of the containers are hydrophobic. Proteins are known to adsorb on to and denature at hydrophobic surface, [4,15] hence we hypothesized that low amounts of protein

might be coating the surface of the tubes due to which the hydrophobic material might be irreversibly denaturing the proteins. ChT has been reported to show a higher affinity for hydrophobic Teflon surfaces than for hydrophilic silica surfaces.[1] At higher protein concentrations, there could be excess protein that has not coated the walls of the microcentrifuge tube which might be providing the major contribution to the Trp/Tyr emission and CD spectra.

To test this hypothesis, we first took a closer look at the denaturation of ChT in plastic tubes as a function of both protein concentration and time of incubation (**Fig. 4b**). We observed that $\Delta\lambda_{max}$ of emission of ChT solution at 10 μg/mL > 20 μg/mL > 100 μg/mL over a 24 h period. The large error bar for some points comes from the experimental setup (see **Fig. 5** for setup), where tubes might end up not experiencing the same force due to their orientation and sample crowding on the weighing boat, which in turn can alter the rate of protein denaturation. Next, we tested the effect of different container materials (hydrophobic *vs*. hydrophilic) on protein denaturation by performing incubation (with agitation) in containers made of polypropylene, Teflon, polystyrene and glass. We observed that chymotrypsin denatured in all 4 different containers (**Fig. S6**), which then shifted our focus to the air-water (A-W) interface.

To test the roles of shaking and A-W interface on ChT denaturation, we set up a 10 μg/mL solution of ChT to incubate in either a plastic or glass container, at different orientations and speed of orbital shaking so that solution flows differently inside the container under two different agitation conditions (see **Fig. 5 b,c** and **Fig. S7** for setup). The solution does not splash in condition 2 regardless of speed of rotation being higher. Even though the shakers move in an orbital fashion, solutions experience agitation in a more orbital shaking manner in condition 2 compared to tube inversion type motion in condition 1. The A-W interfacial area increases under condition 1, relative

to condition 2. Data from fluorescence spectroscopy in **Fig. 5a** show that $\Delta\lambda_{max}$ of protein emission was < 2 nm for condition 2, as opposed to ~ 30 nm red shift in peak maximum for condition 1 after 24 h incubation. Thus, how the solution flows during agitation, and how much of the aqueous solution was exposed to air matters more than material of container used in ChT denaturation.

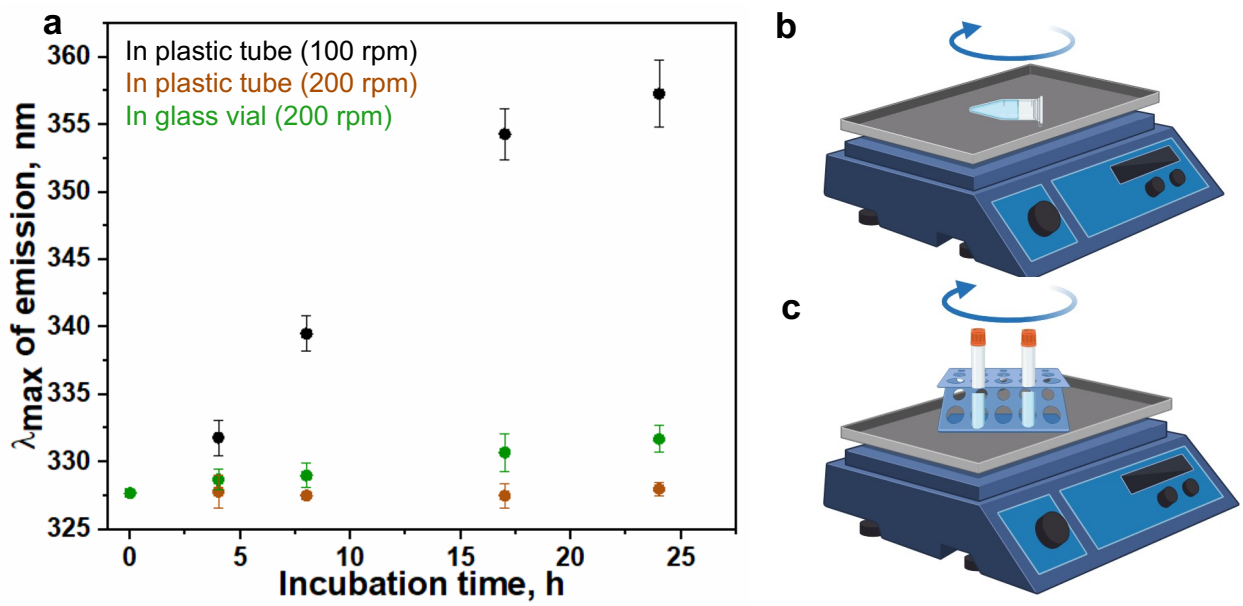

Figure 5. **Effect of container material versus A-W interfacial area in ChT denaturation during agitation.** (a) Change in λ_{max} of emission from fluorescence spectra of 10 µg/mL ChT incubated at 3 different agitation conditions as a function of different incubation times at RT. Samples were in 10 mM sodium phosphate buffer, pH 7.5 filled up to 1 mL in either low protein binding polypropylene microcentrifuge tube or glass vial. Samples were excited at 280 nm. Error bars are from three sample replicates per data point. Schematic representation of the 3 incubation conditions in (a) are shown in (b,c). (b) Samples were in 1.5 mL volume plastic microcentrifuge tubes laid sideways on a shaker set to 100 rpm corresponding to data points in black in (a). (c) Samples were in 15 mL volume plastic centrifuge tubes or 10 mL glass vials set to stand upright on the orbital shaker set to 200 rpm for data points in brown and green in (a). Photos of sample incubation conditions are included in the *SI*. Illustration created in BioRender. Unnikrishnan, M. (2025) https://BioRender.com/m11l861.

To probe the role of the A-W interface further, a side-by-side comparison of samples with and without A-W interface in polypropylene tubes was done by running experiments in parallel.

The A-W interface was removed by filling up the reaction container all the way to the top as shown in **Fig. S8a**. By measuring the intrinsic tryptophan emission of ChT after 24-hour incubation with agitation, it was evident that removing the A-W interface prevents protein denaturation. From **Fig. 6a,** in sample tubes with A-W interface, there is a $\Delta\lambda_{max}$ of 30 nm in the protein emission regardless of the inclusion of NPs in solution. To check for the role of oxidative denaturation, solution was degassed, and ChT samples were prepared in a glove box and tubes sealed so that the air above the protein containing buffer solution is replaced with nitrogen, following which the 24-hour incubation with agitation was performed. The proteins still denatured similarly to when experiments were done with the A-W interface. To further probe the role of oxygen in the air, we experimented with replacing the layer of air with hexanes or decanol - two hydrophobic liquids that are immiscible with the aqueous layer containing protein but is not too viscous to prevent movement of the liquid-liquid interface during agitation (**Fig. S8 b,c**). Emission of Trp/Tyr from sample topped off with hexanes post 24 h incubation with agitation showed that λ_{max} of emission red shifts to a similar extent (**Fig. S8d**) as the control sample with A-W interface (**Fig. S8e**). With decanol, signal from protein emission was too low to be measured in buffer layer.

Addition of surfactants has been shown to prevent protein unfolding and aggregation at the A-W interface.[56] AuNPs have been reported to prevent ChT denaturation at the A-W interface through preferential localization of the nanoparticles at the A-W interface, essentially acting as a surfactant in solution that prevents protein localization at the interface. [57] Adding Tween 20 as a surfactant to reduce protein adsorption at interfaces did prevent denaturation of ChT when agitated at low concentrations (**Fig. 6b**) as observed from changes in λ_{max} of emission of aromatic residues. This confirms that the denaturation of ChT when agitated at low concentrations is a surface-

mediated effect due to adsorption at the A-W interface. Finally, by repeating the 24 h incubation of chymotrypsin and 60-nm AuNP at varying protein:NP ratios and measuring the emission of aromatic residues afterwards (as discussed in **Fig. 3b**), and comparing with and without agitation conditions, we ruled out the role of NPs in denaturation of soft corona and confirmed that there is no red shift in λ_{max} of emission of ChT protein that was exposed to NPs, but was not agitated during incubation (**Fig. 6c**). Note that in a still sample, the surface area of 0.025 nM 60-nm AuNPs is higher than surface areas of air-water interface and interior of the 1.5 mL microcentrifuge tube (see *SI* for calculation).

Thus, enhanced denaturation of ChT protein at low concentrations in solution appears to be due to protein adsorption at a hydrophobic interface such as air-water or hexanes-water, and not due to NPs, and agitation accelerates the process. But is this universal to all proteins, or are some proteins less susceptible than ChT? Response to agitation for proteins has conflicting results in the literature, and hydrodynamic flow-induced protein unfolding and aggregation is thought to be highly dependent on the combination of proteins and interfaces under consideration.[35] Similarly, the rate of protein adsorption at the A-W interface and its tendency to unfold is dependent on structural properties of the protein such as conformational stability and surface hydrophobicity.[15] In a study comparing two proteins, the combined effect of agitation and air-liquid interface caused recombinant human growth hormone (rhGH) to denature whereas recombinant human deoxyribonuclease (rhDNase) was relatively stable due to rhGH being more prone to adsorption at the air-liquid interface.[36] Thus, we used a second model protein to repeat the soft corona studies with AuNPs.

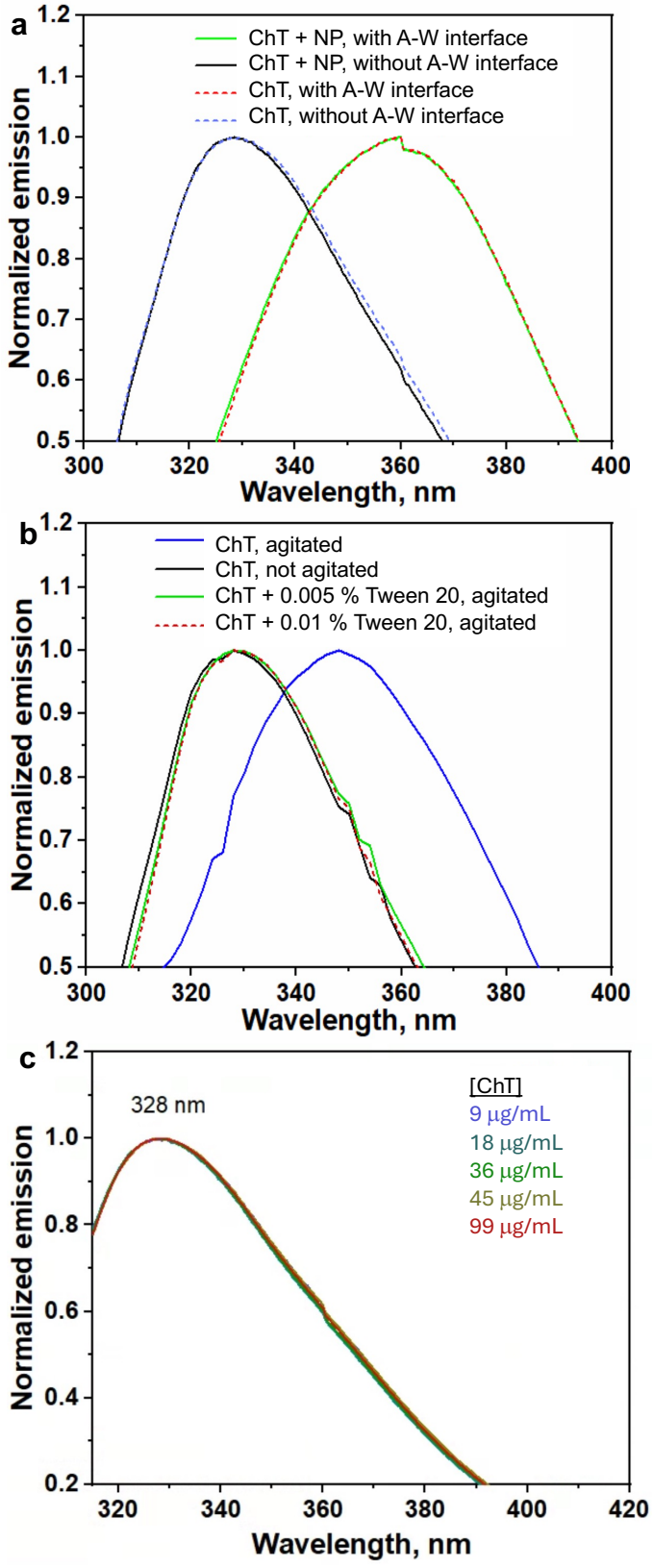
a
ChT + NP, with A-W interface
ChT + NP, without A-W interface
ChT, with A-W interface
ChT, without A-W interface
Normalized emission
Wavelength, nm
b
ChT, agitated
ChT, not agitated
ChT + 0.005 % Tween 20, agitated
ChT + 0.01 % Tween 20, agitated
Normalized emission
Wavelength, nm
c
328 nm
[ChT]
9 µg/mL
18 µg/mL
36 µg/mL
45 µg/mL
99 µg/mL
Normalized emission
Wavelength, nm

Figure 6. **Effect of A-W interface, surfactant and NPs on ChT denaturation.** (a) ChT denaturation after 24 h incubation with agitation at RT with and without the air-water (A-W) interface was measured using Trp/Tyr emission. Sample solutions were incubated in a 2 mL volume polypropylene tube (cap made of same material) filled up to either 1 mL (tube contains an A-W interface) or 2.1 mL (eliminates A-W interface). Across the spectra of 10 μg/mL ChT incubated with 0.025 nM 60-nm NP (green and black lines) and without NPs (red and blue dashed lines), red shift in λ_{max} of emission was observed only in samples with A-W interface (green solid line, red dashed line). (b) Fluorescence emission from 20 μg/mL ChT protein incubated for 24 h at RT with and without addition of surfactant Tween 20. Solution was filled up to 1 mL in 2 mL volume polypropylene tubes (contains A-W interface). Red shift in λ_{max} of emission was observed only in ChT sample agitated without surfactant. Tubes were laid sideways on a shaker set to 200 rpm for incubation with agitation conditions in (a,b). (c) Fluorescence spectra of NP-free ChT supernatant samples post incubation with 0.025 nM 60-nm AuNPs for 24 hours at RT without any agitation. All samples were centrifuged once post incubation to pull down NPs and hard corona proteins, and the supernatant was used to measure emission. Concentration of ChT incubated with NPs was varied between 9-99 mg/mL (legends in graph) in samples. All samples were excited at 280 nm.

A secondary case study using BSA

Serum albumin protein has been extensively investigated in the literature for corona formation on citrate-capped AuNPs. It is the most abundant protein in the circulatory system, that helps maintain the osmotic pressure of blood and acts a multifunctional transporter molecule.[58–61] Bovine serum albumin is a 66 kDa protein with 583 amino acids, and has a net negative charge at pH 7.4. BSA has a prolate ellipsoidal shape with approximate dimensions of 14 nm × 4 nm × 4 nm in aqueous media.[62] The monomeric protein contains 2 tryptophan residues and 20 tyrosine residues (**Fig. 7a**). The secondary structure of BSA is mostly made of helices with a smaller percentage of coils. When BSA protein thermal denaturation is monitored using CD, there is a decrease in peak intensities at higher temperatures (**Fig. S1b, S9**). The fluorescence intensity for the native BSA decreased along with a blue shift in the peak emission wavelength after heat treatment (**Fig. 7b, Fig, S1d**), a spectral change that has been reported previously. This blue shift (338 nm to 324 nm) and low intensity can be due to the change in the local hydrophobicity along with decrease in quantum yield (due to

intramolecular quenching) at increasing temperatures. Irreversible unfolding of α- helices has been reported to start occurring around 52–60°C in BSA, and from 60°C onwards, β aggregation of the molecule begins as unfolding progresses which can cause the aromatic residues to be in a more hydrophobic environment. [61,63,64] BSA also has 10 x more tyrosine residues than tryptophan residues; and as tryptophan emission is quenched at higher temperatures, emission from tyrosine, which is more blue shifted and has lower fluorescence intensity than tryptophan, might be dominating the spectrum. There is a wide range of binding constants reported for BSA adsorption on to AuNPs (K_a = 10^{3}-10^{11} M^{-1}),[53] and three different mechanisms have been proposed to explain this interaction: (i) electrostatic attraction between the positively charged lysine groups of the protein and the anionic citrate layer on the gold surface,[60] (ii) thiol-binding of the cysteine residue directly to the gold surface,[58] and (iii) hydrophobic interaction between the protein and gold surface.[65]

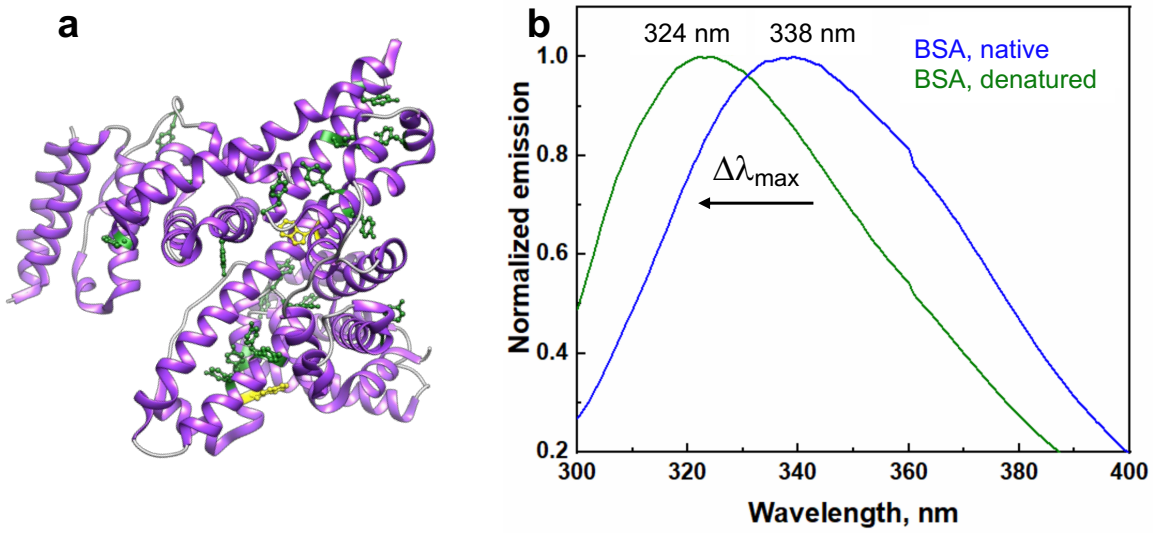

Figure 7. **BSA protein structure and fluorescence spectrum**. Structure of BSA (PDB file 3V03) rendered using Chimera. Helices are shown in purple, and coils in gray. Tryptophan residues are shown in yellow, and tyrosine residues in green. (b) Normalized emission from protein excited at 280 nm before and after thermal denaturation (incubated in 70 °C water bath for 1 h). Samples were cooled down to 20 °C for spectra measurement.

Interaction of BSA with AuNPs

A similar workflow as the 60-nm citrate-AuNPs + chymotrypsin experiment was used to study effect of these NPs on BSA protein denaturation. Initially, there is an increase of ~ 5 nm in D_h upon addition of increasing amount of protein, which remains consistent across a small range of protein concentration (**Fig. 8a**). However, when protein concentration increased to > 50 μg/mL, the D_h continued to increase, and the binding curve did not saturate. The polydispersity index did not increase as the ΔD_h increased however, and the samples did not show aggregation from UV-Vis spectra (**Fig. 8b**). The LSPR peak of the AuNPs showed a slight red shift indicating localization of proteins on the NP surface (**Fig. 8c**). This suggests the formation of multilayers, which BSA protein has been reported to do on citrate capped AuNP surfaces.[66] When a BCA assay (5-250

μg/mL standard curve) was used to quantify the amount of BSA protein adsorbed onto the NPs (hard corona), we found that all of the protein that was added to solution containing NPs could be retrieved in the supernatant once the NPs were pulled down by centrifugation. Since the adsorbed layer can be completely removed by centrifugation, BSA is an ideal "soft corona" protein in our experiments. This data agrees well with previously reported reversible adsorption of BSA on citrate capped AuNPs.[66]

The samples were left to shake gently at RT for 24 hours and then was centrifuged at 13000*g* for 5 mins. The clear supernatant was used to measure BSA emission upon excitation at 280 nm (**Fig. 9a**). A small blue shift of ~ 6 nm in emission maximum was observed at smaller protein: NP ratios (protein concentration 18 μg/mL), which initially suggested that protein denaturation due to NPs can be observed in the soft corona by carefully tuning the protein:NP ratio in the case of BSA. However, the same trend can be observed without the NPs for the same protein concentrations (**Fig. 9b**). Dilution of BSA by itself exhibits a small blue shift in λ_{max} of emission in our measurements and small deviations in λ_{max} of emission has been observed for replicates of the same sample (**Fig. S10**). This can imply a surface-mediated effect, [35] or that this protein assumes a more aggregation-prone monomer conformation at low concentrations.[67] While ChT has not been reported to exhibit the latter behavior, BSA has been reported to assume a more unfolded structure in the 0.05 g/L to 0.20 g/L concentration regime in a 2015 study by Li and colleagues, which can lead to enhanced protein aggregation induced by the gas-liquid interface during foam fractionation. [68] As the concentrations of BSA is in the 0-0.20 g/L regime in our experiments, and $\Delta\lambda_{max}$ of emission is small compared to ChT (~ 6 nm for BSA *vs*. ~ 30 nm for ChT) when the ratio of concentration of protein to A-W interfacial area is reduced, the sensitivity of BSA protein structure

to denature during agitation at low concentrations in a partially filled tube is not apparent from measuring Trp/Tyr emission.

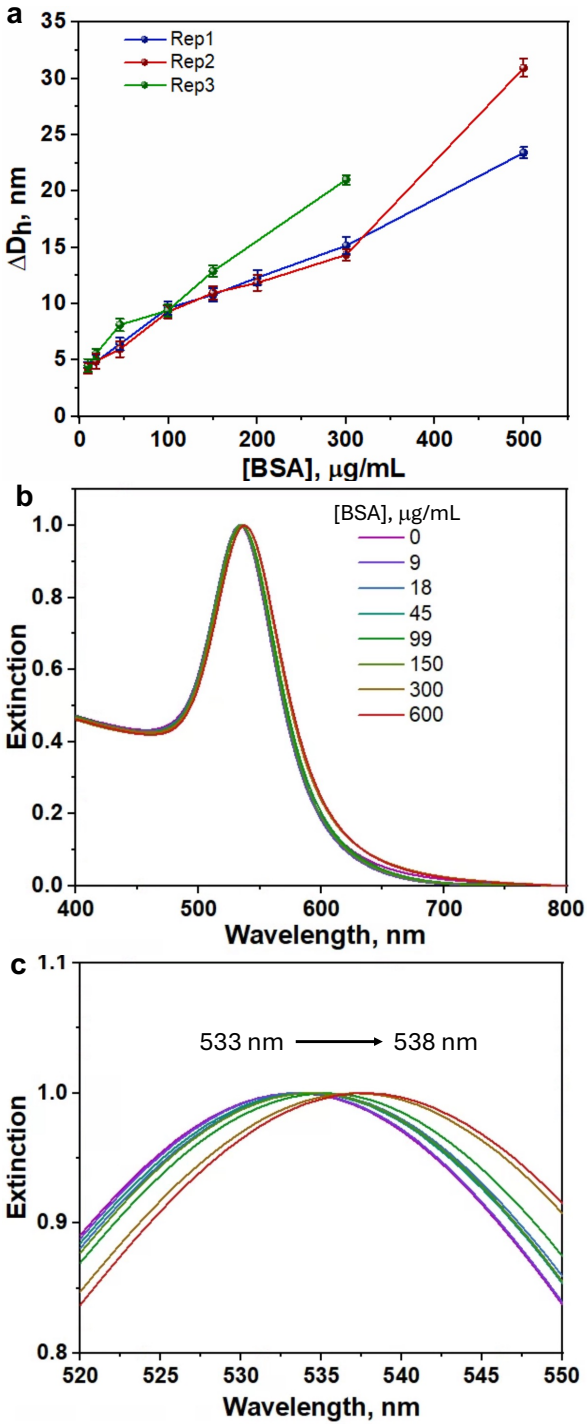

Figure 8. **Soft corona studies of BSA + 60-nm AuNPs.** (a) DLS titration from adding increasing amounts of protein to 0.025 nM NPs in water at pH 6.0. Error bars come from standard deviation of triplicate measurements of same sample on the instrument. Polydispersity index did not increase as the ΔD_h increased with protein concentration. (b) UV-Vis spectra of the NP+protein samples used in (a). There was no aggregation of NPs due to addition of proteins from monitoring extinction (absorbance + scattering) at longer wavelengths. (c) Zoomed in image of the UV-Vis spectra in (b) showing the red shift in LSPR peak of the NPs as proteins coat the NP surface. Concentrations listed in (b) belong to the protein, concentration of NP is 0.025 nM in all samples.

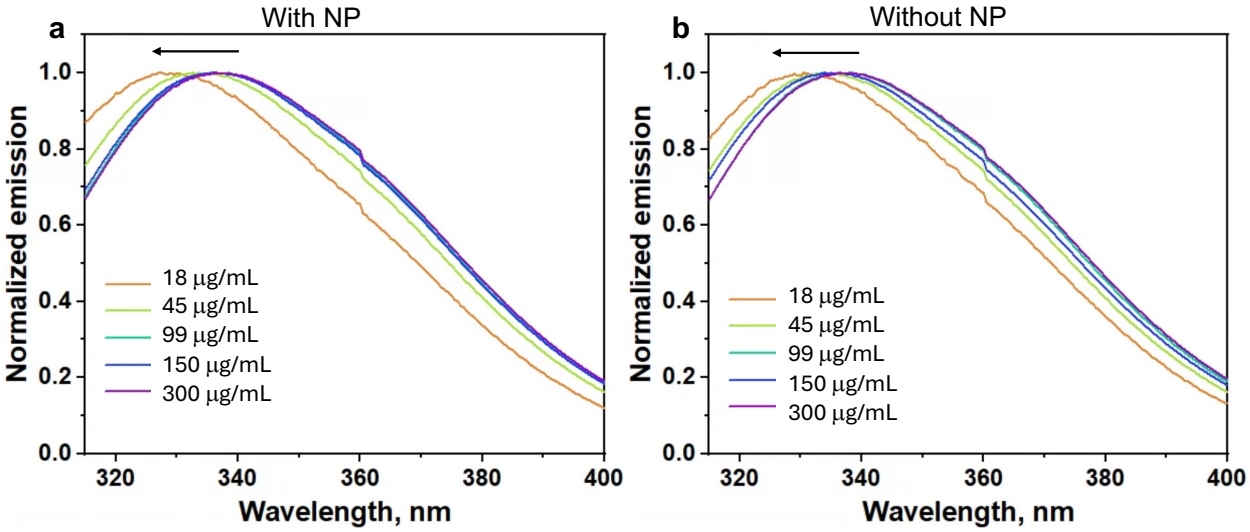

Figure 9. **Fluorescence spectra of NP-free supernatant samples post 24-hour BSA+NP incubation at RT.** BSA was incubated (with agitation) at varying concentrations (a) with 0.025 nM 60-nm AuNPs, and (b) without any nanoparticles. All samples were centrifuged, and the NP-free supernatant was used to measured emission. λ_{max} of emission blue shifted from 337 nm (violet) to 331 nm (orange) as concentration of protein in the tube decreased under both incubation conditions. Samples were incubated in a low protein binding plastic microcentrifuge tube laid sideways on orbital shaker at 100 rpm. Samples were excited at 280 nm.

Chymotrypsin is more sensitive to synergistic effect of A-W interface and agitation during incubation than BSA

Stock solutions of ChT and BSA (typically in the concentration range 500-3000 µg/mL) once thawed, were left to sit or shake at RT along with the protein+NP samples used in our DLS, fluorimeter or CD experiments for the same duration of incubation. For both ChT and BSA

proteins, we observed a minimal shift in λ_{max} of tryptophan emission after 24 h storage at RT at these high concentrations (**Fig. S11**). However, when a low concentration sample of both proteins are vortexed in a tube that is not filled all the way (contains an A-W interface), we observed that the emission peak of ChT visibly red shifts (**Fig. 10a**) while emission peak of BSA does not shift (**Fig. 10b**), indicating that BSA is not as susceptible as chymotrypsin to denaturation at similar incubation conditions.

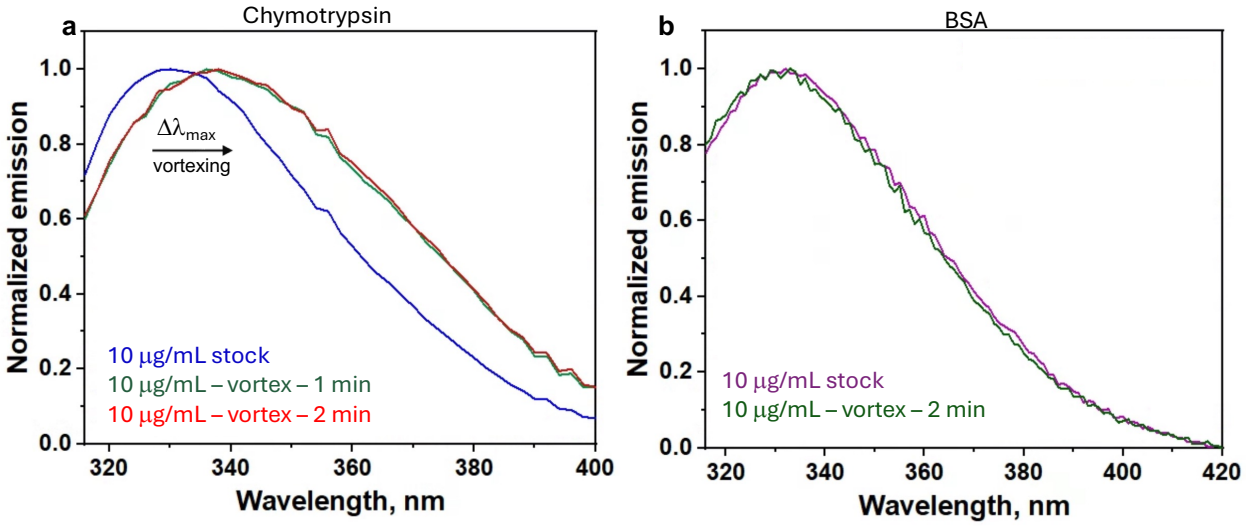

Figure 10. **Synergistic effect of A-W interface and agitation on intrinsic Trp/Tyr emission of ChT *vs.* BSA.** Fluorescence spectra of (a) ChT and (b) BSA protein solutions filled up to 1 mL in 1.5 mL plastic tubes after vortexing indicated a higher sensitivity of ChT proteins to ~~shearing forces~~ agitation in presence of an A-W interface. Samples sat still at RT after vortexing for 24 h before emission was measured by exciting at 280 nm.

It is to be noted that many studies have analyzed the adsorption process of BSA at the A-W interface in detail and looked at the interfacial properties of the protein under different solvent conditions.[69–73] Adsorption of BSA onto an air- water interface (no buffer) has been reported to be reversible from adsorption kinetics studied using surface tension measurements.[73] Interfacial properties of BSA can however be influenced by the presence of surfactants,[71] salts, and protein

concentration.[70] Hofmeister electrolytes has been shown to influence the visco-elastic response of BSA and alter its interfacial activity,[70] hence, buffer composition is an important variable in this field. Hydrogen–deuterium exchange coupled with mass spectrometry (HDX-MS) can help determine the structural changes of BSA protein at the air/water interface in situ at the peptide and amino acid residue level.[69] Using this technique, peptides and residues involved in adsorption of BSA to the A-W interface, and subsequent reduction of helix structures in the unfolding and rearrangement of the interfacial adsorbed BSA were identified. HDX-MS has also been used to correlate structural changes of BSA due to different pH-shifting treatments at the A-W interface with the proteins' foaming properties.[72] Han et al. used interfacial rheology analysis to determine that diffusion-controlled fast adsorption process in a 5 % (m/v) BSA solution in 10 mM PBS (pH 7) took place within 100 s, and that BSA completed structural changes and rearrangement within 2 h of air-water interfacial adsorption.[69] In future studies exploring the competition between the solvent–air interface and the nanoparticle soft corona in protein denaturation, it will be important to employ additional techniques—beyond tryptophan fluorescence as a reporter of local polarity—to obtain more quantitative and comprehensive insights into the molecular and interfacial behavior of proteins across different states: in solution, during adsorption, and at interfaces.

Agitation-induced protein denaturation at the air–water interface during sample preparation should be carefully considered in corona studies, particularly under dilute conditions

Incubation at RT with gentle shaking to facilitate better interaction between NP and protein in the corona has been reported previously.[74,75] In many NP corona papers, however, the

specifications of how the incubation step is conducted (with or without shaking, at what protein concentration, etc.) is not mentioned in the methods section so it is unclear how prevalent this practice is across the various research groups in the field. In a 2022 article by Mohammad-Beigi et al., agitation has been shown to be important in the fibrilization of α-synuclein proteins. In the case of interfacial interactions from polystyrene NPs examined in this study, the in vitro setup was reported to introduce several artificial interfaces like the air-liquid interface and the surfaces of culture well plates or sample tubes. The authors note that these interfaces created a baseline of primary nucleation sites that could differ depending on the product or protein system being studied. Mechanical agitation increased the A-W interface area which aided in speeding up α-synuclein fibril fragmentation.[76] Outside of the NP-protein corona literature, however, the effect of the vapor-liquid interface and agitation on protein stability in solution has been investigated more thoroughly.[35,36,54,56] The synergistic effect of shear and interfaces in causing protein aggregation in solution has been better studied in the context of protein manufacturing for pharmaceutical applications.[35,36] Cryo-electron microscopy data has also shown that reducing protein adsorption at the A-W interface, by using hydrophilized graphene-coated grids which promotes proteins' affinity for the graphene-water interface, prevents protein denaturation arising from contact with air which may occur at any stage of the TEM grid preparation.[77]

It has, however, been shown that responses to agitation and adsorption at interfaces vary for different proteins in these studies. Efforts to categorize proteins as "soft" and "hard" based on degree of conformational stability (resistance to thermal, chemical or shear-induced denaturation), and subsequently identify trends between structural hardness, foamability, and surface hydrophobicity to their affinity for the A-W interfaces have not lead to generalizable framework

due to limited data points.[55,78] ChT has been tagged as a "hard" protein, and BSA as a "soft" protein in the context of rigidity of structure during adsorption processes ,[1,21,79] but ChT underwent significant conformational changes due to adsorption at hydrophobic interfaces in our study. A recent proteome scale study reported that chaperonins, intrinsically disordered proteins and ribosomes were more prone to aggregation under the combined effects of material surface, air-water interface, and agitation. This work by Schvartz et al. showed that the destabilization of proteins exposed to plastic surfaces and their subsequent aggregation at the sheared air/liquid interface could not be prevented even if low protein binding tubes were used. Further, their results on prevention of protein aggregation upon removal of agitation or the air-water interface agrees well with our findings.[54] For agitation-induced reactions, an inverse relationship between protein concentration and denaturation/aggregation in three different monomeric proteins - pegylated megakaryocyte growth and development factor, pegylated granulocyte colony stimulating factor , and osteoprotegerin protein fused at its C-terminus with the sequence from the Fc portion from an immunoglobulin – have been explained using the A-W interface as the rate-limiting reagent. [56] Hence, the air–water interface and agitation may play significant roles in corona studies involving proteins beyond chymotrypsin, and appropriate control experiments should be conducted to accurately attribute effects to the nanoparticle surface.

CONCLUSION

In this work, we explored the differential effects of citrate-capped AuNPs and interfacial agitation on two model proteins, chymotrypsin (ChT) and bovine serum albumin (BSA), within the context

of soft corona formation. In soft corona studies, maintaining a low protein-to-NP ratio ensures that data primarily reflects protein-NP interactions rather than excess free protein in solution. However, when the ratio of protein to NP is reduced, the ratio of protein to air-liquid interface and to area of container walls is also reduced. For certain proteins like chymotrypsin, adsorption at the hydrophobic air-water interface can cause denaturation, and the continuous renewal of this interfacial area due to agitation can accelerate the denaturation reaction. This leads to an inverse relationship between protein concentration and denaturation—a surface-mediated effect that could be mistakenly attributed to protein–nanoparticle interactions. In the absence of agitation or adsorption to the A-W interface, chymotrypsin protein desorption from the NP surface in a permanently denatured form does not appear to be a major downstream effect when exposed to citrate-capped AuNPs. BSA protein on the other hand did not exhibit significant denaturation in the soft corona of AuNPs, even under agitation and in the presence of an air–water interface, as indicated by intrinsic tryptophan and tyrosine fluorescence measurements. This highlights the protein-specific nature of interfacial denaturation, with the propensity to unfold at the air–water interface varying between different proteins.

In the workflow where incubation of protein and NP together is followed by isolation of soft corona protein for characterization, the source of protein denaturation must be unambiguously identified for the research to be meaningful in corona studies. For chymotrypsin, avoiding air-water interfaces or agitation could prevent synergistic denaturation effects at concentrations below 50 μg/mL over a 24-hour incubation period in our experimental setup. This threshold may rise with factors such as reduced solution volume, increased agitation speed, mode of agitation (change in A-W interfacial area), or prolonged/high-temperature incubation. We recommend that when performing corona studies at low protein concentrations (μg/mL or lower, although this value is

subjective on incubation parameters), in addition to protein alone control experiments, eliminating the air-water interfaces by filling tubes all the way and ensuring air bubbles do not form would help avoid spurious sources of protein denaturation. Alternatively, lowering protein affinity for air-water interfaces compared to NP surfaces—for example, by adding surface tension-reducing agents—can help ensure data reflects bulk protein-NP interactions. As creation of interfaces in an experimental setup is inevitable, and many more surfaces beside that of the NP surface become available for the protein to adsorb onto, contribution from these interfaces needs to be accounted for in corona studies.

ASSOCIATED CONTENT

Supporting Information. The Supporting Information is available free of charge.

Surface area calculations, Thermal melt spectra of proteins, TEM images of AuNPs, additional DLS titrations of ChT and AuNP, BCA assay standard curve for ChT, corona formation studies of ChT with 40-nm AuNPs, Trp/Tyr emission studies for effect of temperature and agitation on concentration-dependent ChT denaturation, Trp/Tyr emission studies for effect of container material on ChT denaturation, photos of incubation condition setups, Trp/Tyr emission studies for monitoring ChT denaturation with and without the A-W interface, CD data for BSA, fluorescence spectra of BSA at dilute concentrations, Trp/Tyr emission spectra of protein stocks kept still at high concentrations. (PDF)

AUTHOR INFORMATION

Corresponding Author

* Catherine J. Murphy - Department of Chemistry, University of Illinois Urbana-Champaign, Urbana, IL 61801, USA. Email: murphycj@illinois.edu. ORCID ID: 0000-0001-7066-5575.

Authors

Mahima Unnikrishnan - Department of Chemistry, University of Illinois Urbana-Champaign, Urbana, IL 61801, USA. Email: mahima@illinois.edu. ORCID ID: 0000-0003-2530-7036.

Martin Gruebele - Department of Chemistry, University of Illinois Urbana-Champaign, Urbana, IL 61801, USA. Email: mgruebel@illinois.edu. ORCID ID: 0000-0001-9291-8123.

Author Contributions

M.U. performed research. C.J.M. and M.G. supervised research. The manuscript was written through contributions from all authors. All authors have given approval to the final version of the manuscript.

Funding Sources

Contributions from M.U. and C.J.M. were supported by the National Science Foundation under Grant No. CHE-2001611, the NSF Center for Sustainable Nanotechnology. Contributions from M.G. were supported by the National Science Foundation under Grant No. MCB 2205665.

Notes

The authors declare no competing financial interest.

ACKNOWLEDGMENT

Electron microscopy was carried out at the Frederick Seitz Materials Research Laboratory Central Research Facilities, University of Illinois at Urbana-Champaign. Illustrations were created with

BioRender. We thank Dr. Kyoungtea Kim and Dr. Michael P. Schwartz for helpful discussions, and the reviewers for helpful comments.

ABBREVIATIONS

ChT, alpha-chymotrypsin; BSA, bovine serum albumin; A-W interface, air-water interface; RT, room temperature.

REFERENCES

(1) Nakanishi, K.; Sakiyama, T.; Imamura, K. On the Adsorption of Proteins on Solid Surfaces, a Common but Very Complicated Phenomenon. *J Biosci Bioeng* **2001**, *91* (3), 233–244. https://doi.org/10.1016/S1389-1723(01)80127-4.

(2) Walkey, C. D.; Chan, W. C. W. Understanding and Controlling the Interaction of Nanomaterials with Proteins in a Physiological Environment. *Chem Soc Rev* **2012**, *41* (7), 2780–2799. https://doi.org/10.1039/c1cs15233e.

(3) Norde, W. Adsorption of Proteins from Solution at the Solid-Liquid Interface. *Adv Colloid Interface Sci* **1986**, *25* (C), 267–340. https://doi.org/10.1016/0001-8686(86)80012-4.

(4) Rabe, M.; Verdes, D.; Seeger, S. Understanding Protein Adsorption Phenomena at Solid Surfaces. *Adv Colloid Interface Sci* **2011**, *162* (1–2), 87–106. https://doi.org/10.1016/j.cis.2010.12.007.

(5) Onuchic, J. N.; Wolynes, P. G. Theory of Protein Folding. *Curr Opin Struct Biol* **2004**, *14* (1), 70–75. https://doi.org/10.1016/j.sbi.2004.01.009.

(6) Plotkin, S. S.; Onuchic, J. N. Understanding Protein Folding with Energy Landscape Theory. Part I: Basic Concepts. *Q Rev Biophys* **2002**, *35* (2), 111–167. https://doi.org/10.1017/S0033583502003761.

(7) Gruebele, M. Downhill Protein Folding: Evolution Meets Physics. *C R Biol* **2005**, *328* (8), 701–712. https://doi.org/10.1016/j.crvi.2005.02.007.

(8) Gruebele, M.; Dave, K.; Sukenik, S. Globular Protein Folding In Vitro and In Vivo. *Annu Rev Biophys* **2016**, *45*, 233–251. https://doi.org/10.1146/annurev-biophys-062215-011236.

(9) You, C. C.; De, M.; Han, G.; Rotello, V. M. Tunable Inhibition and Denaturation of α-Chymotrypsin with Amino Acid-Functionalized Gold Nanoparticles. *J Am Chem Soc* **2005**, *127* (37), 12873–12881. https://doi.org/10.1021/ja0512881.

(10) You, C. C.; De, M.; Rotello, V. M. Contrasting Effects of Exterior and Interior Hydrophobic Moieties in the Complexation of Amino Acid Functionalized Gold Clusters with α-Chymotrypsin. *Org Lett* **2005**, *7* (25), 5685–5688. https://doi.org/10.1021/ol052367k.

(11) Slack, S. M.; Horbett, T. A. The Vroman Effect: A Critical Review. In *Proteins at Interfaces II, 1st ed.; ACS Symposium Series*; 1995; Vol. 602, pp 112–128. https://doi.org/10.1021/bk-1995-0602.ch008.

(12) Vroman, L.; Adams, A. L. J. Identification of Rapid Changes at Plasma–Solid Interfaces. *J Biomed Mater Res* **1969**, *3* (1), 43. https://doi.org/10.1002/jbm.820030106.

(13) Wolfram, J.; Yang, Y.; Shen, J.; Moten, A.; Chen, C.; Shen, H.; Ferrari, M.; Zhao, Y. The Nano-Plasma Interface: Implications of the Protein Corona. *Colloids Surf B Biointerfaces* **2014**, *124* (11), 17–24. https://doi.org/10.1016/j.colsurfb.2014.02.035.

(14) Pan, H.; Qin, M.; Meng, W.; Cao, Y.; Wang, W. How Do Proteins Unfold upon Adsorption on Nanoparticle Surfaces? *Langmuir* **2012**, *28* (35), 12779–12787. https://doi.org/10.1021/la302258k.

(15) Yano, Y. F. Kinetics of Protein Unfolding at Interfaces. *Journal of Physics Condensed Matter* **2012**, *24* (50), 503101. https://doi.org/10.1088/0953-8984/24/50/503101.

(16) Cedervall, T.; Lynch, I.; Lindman, S.; Berggård, T.; Thulin, E.; Nilsson, H.; Dawson, K. A.; Linse, S. Understanding the Nanoparticle-Protein Corona Using Methods to Quntify Exchange Rates and Affinities of Proteins for Nanoparticles. *Proc Natl Acad Sci U S A* **2007**, *104* (7), 2050–2055. https://doi.org/10.1073/pnas.0608582104.

(17) Cedervall, T.; Lynch, I.; Foy, M.; Berggård, T.; Donnelly, S. C.; Cagney, G.; Linse, S.; Dawson, K. A. Detailed Identification of Plasma Proteins Adsorbed on Copolymer Nanoparticles. *Angewandte Chemie - International Edition* **2007**, *46* (30), 5754–5756. https://doi.org/10.1002/anie.200700465.

(18) García-álvarez, R.; Vallet-Regí, M. Hard and Soft Protein Corona of Nanomaterials: Analysis and Relevance. *Nanomaterials* **2021**, *11* (4), 888. https://doi.org/10.3390/nano11040888.

(19) Milani, S.; Baldelli Bombelli, F.; Pitek, A. S.; Dawson, K. A.; Rädler, J. Reversible versus Irreversible Binding of Transferrin to Polystyrene Nanoparticles: Soft and Hard Corona. *ACS Nano* **2012**, *6* (3), 2532–2541. https://doi.org/10.1021/nn204951s.

(20) Hoang, K. N. L.; Wheeler, K. E.; Murphy, C. J. Isolation Methods Influence the Protein Corona Composition on Gold-Coated Iron Oxide Nanoparticles. *Anal Chem* **2022**, *94* (11), 4737–4746. https://doi.org/10.1021/acs.analchem.1c05243.

(21) Kondo, A.; Oku, S.; Murakami, F.; Higashitani, K. Conformational Changes in Protein Molecules upon Adsorption on Ultrafine Particles. *Colloids Surf B Biointerfaces* **1993**, *1* (3), 197–201. https://doi.org/10.1016/0927-7765(93)80051-Y.

(22) Kharazian, B.; Lohse, S. E.; Ghasemi, F.; Raoufi, M.; Saei, A. A.; Hashemi, F.; Farvadi, F.; Alimohamadi, R.; Jalali, S. A.; Shokrgozar, M. A.; Hadipour, N. L.; Ejtehadi, M. R.;

Mahmoudi, M. Bare Surface of Gold Nanoparticle Induces Inflammation through Unfolding of Plasma Fibrinogen. *Sci Rep* **2018**, *8* (1), 1–9. https://doi.org/10.1038/s41598-018-30915-7.

(23) Fleischer, C. C.; Payne, C. K. Nanoparticle-Cell Interactions: Molecular Structure of the Protein Corona and Cellular Outcomes. *Acc Chem Res* **2014**, *47* (8), 2651–2659. https://doi.org/10.1021/ar500190q.

(24) Glomm, W. R.; Halskau, Ø.; Hanneseth, A. M. D.; Volden, S. Adsorption Behavior of Acidic and Basic Proteins onto Citrate-Coated Au Surfaces Correlated to Their Native Fold, Stability, and PI. *Journal of Physical Chemistry B* **2007**, *111* (51), 14329–14345. https://doi.org/10.1021/jp074839d.

(25) Shang, W.; Nuffer, J. H.; Dordick, J. S.; Siegel, R. W. Unfolding of Ribonuclease a on Silica Nanoparticle Surfaces. *Nano Lett* **2007**, *7* (7), 1991–1995. https://doi.org/10.1021/nl070777r.

(26) Sanchez-Guzman, D.; Giraudon-Colas, G.; Marichal, L.; Boulard, Y.; Wien, F.; Degrouard, J.; Baeza-Squiban, A.; Pin, S.; Renault, J. P.; Devineau, S. In Situ Analysis of Weakly Bound Proteins Reveals Molecular Basis of Soft Corona Formation. *ACS Nano* **2020**, *14* (7), 9073–9088. https://doi.org/10.1021/acsnano.0c04165.

(27) Mohammad-Beigi, H.; Hayashi, Y.; Zeuthen, C. M.; Eskandari, H.; Scavenius, C.; Juul-Madsen, K.; Vorup-Jensen, T.; Enghild, J. J.; Sutherland, D. S. Mapping and Identification of Soft Corona Proteins at Nanoparticles and Their Impact on Cellular Association. *Nat Commun* **2020**, *11* (1), 4535. https://doi.org/10.1038/s41467-020-18237-7.

(28) Kari, O. K.; Ndika, J.; Parkkila, P.; Louna, A.; Lajunen, T.; Puustinen, A.; Viitala, T.; Alenius, H.; Urtti, A. In Situ Analysis of Liposome Hard and Soft Protein Corona Structure and Composition in a Single Label-Free Workflow. *Nanoscale* **2020**, *12* (3), 1728–1741. https://doi.org/10.1039/c9nr08186k.

(29) Riley, M. B.; Strandquist, E.; Weitzel, C. S.; Driskell, J. D. Structure and Activity of Native and Thiolated α-Chymotrypsin Adsorbed onto Gold Nanoparticles. *Colloids Surf B Biointerfaces* **2022**, *220*, 112867. https://doi.org/10.1016/j.colsurfb.2022.112867.

(30) Fischer, N. O.; McIntosh, C. M.; Simard, J. M.; Rotello, V. M. Inhibition of Chymotrypsin through Surface Binding Using Nanoparticle-Based Receptors. *Proc Natl Acad Sci U S A* **2002**, *99* (8), 5018–5023. https://doi.org/10.1073/pnas.082644099.

(31) In¨aki Guijarro, J.; Sunde, M.; Jones, J. A.; Campbelli, I. D.; Dobson, C. M. Amyloid Fibril Formation by an SH3 Domain. *Proc Natl Acad Sci U S A* **1998**, *95* (8), 4224–4228. https://doi.org/10.1073/pnas.95.8.4224.

(32) Swaminathan, R.; Ravi, V. K.; Kumar, S.; Kumar, M. V. S.; Chandra, N. Lysozyme: A Model Protein for Amyloid Research. In *Advances in Protein Chemistry and Structural Biology*; 2011; Vol. 84, pp 63–111. https://doi.org/10.1016/B978-0-12-386483-3.00003-3.

(33) Chiti, F.; Webster, P.; Taddei, N.; Clark, A.; Stefani, M.; Ramponi, G.; Dobson, C. M. Designing Conditions for in Vitro Formation of Amyloid Protofilaments and Fibrils. *Proc Natl Acad Sci U S A* **1999**, *96* (7), 3590–3594. https://doi.org/10.1073/pnas.96.7.3590.

(34) Fändrich, M.; Fletcher, M. A.; Dobson, C. M. Amyloid Fibrils from Muscle Myoglobin. *Nature* **2001**, *410* (6825), 165–166. https://doi.org/10.1038/35065514.

(35) Grigolato, F.; Arosio, P. Synergistic Effects of Flow and Interfaces on Antibody Aggregation. *Biotechnol Bioeng* **2020**, *117* (2), 417–428. https://doi.org/10.1002/bit.27212.

(36) Maa, Y. F.; Hsu, C. C. Protein Denaturation by Combined Effect of Shear and Air-Liquid Interface. *Biotechnol Bioeng* **1997**, *54* (6), 503–512. https://doi.org/10.1002/(SICI)1097-0290(19970620)54:6<503::AID-BIT1>3.0.CO;2-N.

(37) Gerhardt, A.; McGraw, N. R.; Schwartz, D. K.; Bee, J. S.; Carpenter, J. F.; Randolph, T. W. Protein Aggregation and Particle Formation in Prefilled Glass Syringes. *J Pharm Sci* **2014**, *103* (6), 1601–1612. https://doi.org/10.1002/jps.23973.

(38) Bee, J. S.; Schwartz, D. K.; Trabelsi, S.; Freund, E.; Stevenson, J. L.; Carpenter, J. F.; Randolph, T. W. Production of Particles of Therapeutic Proteins at the Air-Water Interface during Compression/Dilation Cycles. *Soft Matter* **2012**, *8* (40), 10329–10335. https://doi.org/10.1039/c2sm26184g.

(39) Wood, C. V.; Razinkov, V. I.; Qi, W.; Furst, E. M.; Roberts, C. J. A Rapid, Small-Volume Approach to Evaluate Protein Aggregation at Air-Water Interfaces. *J Pharm Sci* **2021**, *110* (3), 1083–1092.

(40) Wood, C. V.; Razinkov, V. I.; Qi, W.; Roberts, C. J.; Vermant, J.; Furst, E. M. Antibodies Adsorbed to the Air-Water Interface Form Soft Glasses. *Langmuir* **2023**, *39* (22), 7775–7782. https://doi.org/10.1021/acs.langmuir.3c00616.

(41) Gerhardt, A.; McUmber, A. C.; Nguyen, B. H.; Lewus, R.; Schwartz, D. K.; Carpenter, J. F.; Randolph, T. W. Surfactant Effects on Particle Generation in Antibody Formulations in Pre-Filled Syringes. *J Pharm Sci* **2015**, *104* (12), 4056–4064. https://doi.org/10.1002/jps.24654.

(42) Liu, L.; Qi, W.; Schwartz, D. K.; Randolph, T. W.; Carpenter, J. F. The Effects of Excipients on Protein Aggregation during Agitation: An Interfacial Shear Rheology Study. *J Pharm Sci* **2013**, *102* (8), 2460–2470. https://doi.org/10.1002/jps.23622.

(43) Deng, J.; Davies, D. R.; Wisedchaisri, G.; Wu, M.; Hol, W. G. J.; Mehlin, C. An Improved Protocol for Rapid Freezing of Protein Samples for Long-Term Storage. *Acta Crystallogr D Biol Crystallogr* **2004**, *60* (1), 203–204. https://doi.org/10.1107/S0907444903024491.

(44) Pikal-Cleland, K. A.; Rodríguez-Hornedo, N.; Amidon, G. L.; Carpenter, J. F. Protein Denaturation during Freezing and Thawing in Phosphate Buffer Systems: Monomeric and Tetrameric β-Galactosidase. *Arch Biochem Biophys* **2000**, *384* (2), 398–406. https://doi.org/10.1006/abbi.2000.2088.

(45) Perrault, S. D.; Chan, W. C. W. Synthesis and Surface Modification of Highly Monodispersed, Spherical Gold Nanoparticles of 50-200 Nm. *J Am Chem Soc* **2009**, *131* (47), 17042–17043. https://doi.org/10.1021/ja907069u.

(46) Micsonai, A.; Wien, F.; Kernya, L.; Lee, Y. H.; Goto, Y.; Réfrégiers, M.; Kardos, J. Accurate Secondary Structure Prediction and Fold Recognition for Circular Dichroism Spectroscopy. *Proc Natl Acad Sci U S A* **2015**, *112* (24), E3095–E3103. https://doi.org/10.1073/pnas.1500851112.

(47) Hanlon, A. D.; Larkin, M. I.; Reddick, R. M. Free-Solution, Label-Free Protein-Protein Interactions Characterized by Dynamic Light Scattering. *Biophys J* **2010**, *98* (2), 297–304. https://doi.org/10.1016/j.bpj.2009.09.061.

(48) Chen, Y.; Barkley, M. D. Toward Understanding Tryptophan Fluorescence in Proteins. *Biochemistry* **1998**, *37* (28), 9976–9982. https://doi.org/10.1021/bi980274n.

(49) Gorinstein, S.; Goshev, I.; Moncheva, S.; Zemser, M.; Weisz, M.; Caspi, A.; Libman, I.; Lerner, H. T.; Trakhtenberg, S.; Martín-Belloso, O. Intrinsic Tryptophan Fluorescence of Human Serum Proteins and Related Conformational Changes. *J Protein Chem* **2000**, *19* (8), 637–642. https://doi.org/10.1023/A:1007192017291.

(50) Burstein, E.; Vedenkina, N.; Ivkova, M. Fluorescence and the Location of Tryptophan Residues in Protein Molecules. *Photochem Photobiol* **1973**, *18* (4), 263–279. https://doi.org/10.1111/j.1751-1097.1973.tb06422.x.

(51) De Diego, T.; Lozano, P.; Gmouh, S.; Vaultier, M.; Iborra, J. L. Fluorescence and CD Spectroscopic Analysis of the α-Chymotrypsin Stabilization by the Ionic Liquid, 1-Ethyl-3-Methylimidazolium Bis[(Trifluoromethyl)Sulfonyl]Amide. *Biotechnol Bioeng* **2004**, *88* (7), 916–924. https://doi.org/10.1002/bit.20330.

(52) García-Álvarez, R.; Hadjidemetriou, M.; Sánchez-Iglesias, A.; Liz-Marzán, L. M.; Kostarelos, K. In Vivo Formation of Protein Corona on Gold Nanoparticles. The Effect of Their Size and Shape. *Nanoscale* **2018**, *10* (3), 1256–1264. https://doi.org/10.1039/c7nr08322j.

(53) Dennison, J. M.; Zupancic, J. M.; Lin, W.; Dwyer, J. H.; Murphy, C. J. Protein Adsorption to Charged Gold Nanospheres as a Function of Protein Deformability. *Langmuir* **2017**, *33* (31), 7751–7761. https://doi.org/10.1021/acs.langmuir.7b01909.

(54) Schvartz, M.; Saudrais, F.; Devineau, S.; Aude, J. C.; Chédin, S.; Henry, C.; Millán-Oropeza, A.; Perrault, T.; Pieri, L.; Pin, S.; Boulard, Y.; Brotons, G.; Renault, J. P. A Proteome Scale Study Reveals How Plastic Surfaces and Agitation Promote Protein Aggregation. *Sci Rep* **2023**, *13* (1), 1–17. https://doi.org/10.1038/s41598-023-28412-7.

(55) Tripp, B. C.; Magda, J. J.; Andrade, J. D. Adsorption of Globular Proteins at the Air/Water Interface as Measured via Dynamic Surface Tension: Concentration Dependence, Mass-Transfer Considerations, and Adsorption Kinetics. *J Colloid Interface Sci* **1995**, *173* (1), 16–27. https://doi.org/10.1006/jcis.1995.1291.

(56) Treuheit, M. J.; Kosky, A. A.; Brems, D. N. Inverse Relationship of Protein Concentration and Aggregation. *Pharm Res* **2002**, *19* (4), 511–516. https://doi.org/10.1023/A:1015108115452.

(57) Jordan, B. J.; Hong, R.; Gider, B.; Hill, J.; Emrick, T.; Rotello, V. M. Stabilization of α-Chymotrypsin at Air-Water Interface through Surface Binding to Gold Nanoparticle Scaffolds. *Soft Matter* **2006**, *2* (7), 558–560. https://doi.org/10.1039/b603980d.

(58) Tsai, D. H.; Delrio, F. W.; Keene, A. M.; Tyner, K. M.; MacCuspie, R. I.; Cho, T. J.; Zachariah, M. R.; Hackley, V. A. Adsorption and Conformation of Serum Albumin Protein on Gold Nanoparticles Investigated Using Dimensional Measurements and in Situ Spectroscopic Methods. *Langmuir* **2011**, *27* (6), 2464–2477. https://doi.org/10.1021/la104124d.

(59) Chakraborty, S.; Joshi, P.; Shanker, V.; Ansari, Z. A.; Singh, S. P.; Chakrabarti, P. Contrasting Effect of Gold Nanoparticles and Nanorods with Different Surface Modifications on the Structure and Activity of Bovine Serum Albumin. *Langmuir* **2011**, *27* (12), 7722–7731. https://doi.org/10.1021/la200787t.

(60) Brewer, S. H.; Glomm, W. R.; Johnson, M. C.; Knag, M. K.; Franzen, S. Probing BSA Binding to Citrate-Coated Gold Nanoparticles and Surfaces. *Langmuir* **2005**, *21* (20), 9303–9307. https://doi.org/10.1021/la050588t.

(61) Rahul, C.; Susan, B.; Sangram, R.; Sunil, S.; Julian, B.; Zygmunt, G.; Ignacy, G. Effect of Quencher, Denaturants, Temperature and PH on the Fluorescent Properties of BSA Protected Gold Nanoclusters. *J Lumin* **2015**, *168*, 62–68. https://doi.org/10.1016/j.jlumin.2015.07.030.

(62) Wright, A. K.; Thompson, M. R. Hydrodynamic Structure of Bovine Serum Albumin Determined by Transient Electric Birefringence. *Biophys J* **1975**, *15* (2), 137–141. https://doi.org/10.1016/S0006-3495(75)85797-3.

(63) Borzova, V. A.; Markossian, K. A.; Chebotareva, N. A.; Kleymenov, S. Y.; Poliansky, N. B.; Muranov, K. O.; Stein-Margolina, V. A.; Shubin, V. V.; Markov, D. I.; Kurganov, B. I. Kinetics of Thermal Denaturation and Aggregation of Bovine Serum Albumin. *PLoS One* **2016**, *11* (4), e0153495. https://doi.org/10.1371/JOURNAL.PONE.0153495.

(64) Sahin, Z.; Demir, Y. K.; Kayser, V. Global Kinetic Analysis of Seeded BSA Aggregation. *European Journal of Pharmaceutical Sciences* **2016**, *86*, 115–124. https://doi.org/10.1016/j.ejps.2016.03.007.

(65) Dominguez-Medina, S.; Blankenburg, J.; Olson, J.; Landes, C. F.; Link, S. Adsorption of a Protein Monolayer via Hydrophobic Interactions Prevents Nanoparticle Aggregation under Harsh Environmental Conditions. *ACS Sustain Chem Eng* **2013**, *1* (7), 833–842. https://doi.org/10.1021/sc400042h.

(66) Mishra, A.; Das, P. K. Thermodynamics of Multilayer Protein Adsorption on a Gold Nanoparticle Surface. *Physical Chemistry Chemical Physics* **2022**, *24* (37), 22464–22476. https://doi.org/10.1039/d2cp02439j.

(67) Zhang, C.; Bye, J. W.; Lui, L. H.; Zhang, H.; Hales, J.; Brocchini, S.; Curtis, R. A.; Dalby, P. A. Enhanced Thermal Stability and Reduced Aggregation in an Antibody Fab Fragment at Elevated Concentrations. *Mol Pharm* **2023**, *20* (5), 2650–2661. https://doi.org/10.1021/acs.molpharmaceut.3c00081.

(68) Li, R.; Fu, N.; Wu, Z.; Wang, Y.; Wang, Y. Protein Aggregation in Foam Fractionation of Bovine Serum Albumin: Effect of Protein Concentration. *Biochem Eng J* **2015**, *103*, 234–241. https://doi.org/10.1016/j.bej.2015.08.006.

(69) Han, F.; Shen, Q.; Zheng, W.; Zuo, J.; Zhu, X.; Li, J.; Peng, C.; Li, B.; Chen, Y. The Conformational Changes of Bovine Serum Albumin at the Air/Water Interface: HDX-MS and Interfacial Rheology Analysis. *Foods* **2023**, *12* (8), 1601. https://doi.org/10.3390/foods12081601.

(70) Lakshmanan, M.; Dhathathreyan, A.; Miller, R. Synergy between Hofmeister Effect and Coupled Water in Proteins: Unusual Dilational Moduli of BSA at Air/Solution Interface. *Colloids Surf A Physicochem Eng Asp* **2008**, *324* (1–3), 194–201. https://doi.org/10.1016/j.colsurfa.2008.04.014.

(71) Rodríguez Niño, M. R.; Rodríguez Patino, J. M. Surface Tension of Bovine Serum Albumin and Tween 20 at the Air-Aqueous Interface. *J Am Oil Chem Soc* **1998**, *75* (10), 1241–1248. https://doi.org/10.1007/s11746-998-0169-6.

(72) Yang, C.; Han, F.; Wang, Z.; Cui, B.; Wu, Y.; Shen, Q.; Li, B.; Chen, Y. The Air-Water Interfacial Properties of Bovine Serum Albumin with PH-Shifting Treatments by Hydrogen-Deuterium Exchange Mass Spectrometry. *Food Hydrocoll* **2025**, *166*, 111360. https://doi.org/10.1016/j.foodhyd.2025.111360.

(73) Thi-Yen Le, T.; Hussain, S.; Tsay, R. Y.; Lin, S. Y. On the Adsorption Kinetics of Bovine Serum Albumin at the Air–Water Interface. *J Mol Liq* **2022**, *353*, 118813. https://doi.org/10.1016/j.molliq.2022.118813.

(74) Bae, S. H.; Yu, J.; Lee, T. G.; Choi, S. J. Protein Food Matrix–ZnO Nanoparticle Interactions Affect Protein Conformation, but May Not Be Biological Responses. *Int J Mol Sci* **2018**, *19* (12), 10–12. https://doi.org/10.3390/ijms19123926.

(75) Liu, S.; Jiang, X.; Tian, X.; Wang, Z.; Xing, Z.; Chen, J.; Zhang, J.; Wang, C.; Dong, L. A Method to Measure the Denatured Proteins in the Corona of Nanoparticles Based on the Specific Adsorption of Hsp90ab1. *Nanoscale* **2020**, *12* (29), 15857–15868. https://doi.org/10.1039/d0nr02297g.

(76) Mohammad-Beigi, H.; Zanganeh, M.; Scavenius, C.; Eskandari, H.; Farzadfard, A.; Shojaosadati, S. A.; Enghild, J. J.; Otzen, D. E.; Buell, A. K.; Sutherland, D. S. A Protein Corona Modulates Interactions of α-Synuclein with Nanoparticles and Alters the Rates of the Microscopic Steps of Amyloid Formation. *ACS Nano* **2022**, *16* (1), 1102–1118. https://doi.org/10.1021/acsnano.1c08825.

(77) D'Imprima, E.; Floris, D.; Joppe, M.; Sánchez, R.; Grininger, M.; Kühlbrandt, W. Protein Denaturation at the Air-Water Interface and How to Prevent It. *Elife* **2019**, *8*, 1–18. https://doi.org/10.7554/eLife.42747.

(78) Stellwagen, E.; Wilgus, H. Relationship of Protein Thermostability to Accessible Surface Area. *Nature* **1978**, *275* (5678), 342–343. https://doi.org/10.1038/275342a0.

(79) Demanèche, S.; Chapel, J. P.; Monrozier, L. J.; Quiquampoix, H. Dissimilar PH-Dependent Adsorption Features of Bovine Serum Albumin and α-Chymotrypsin on Mica Probed by AFM. *Colloids Surf B Biointerfaces* **2009**, *70* (2), 226–231. https://doi.org/10.1016/j.colsurfb.2008.12.036.

TOC

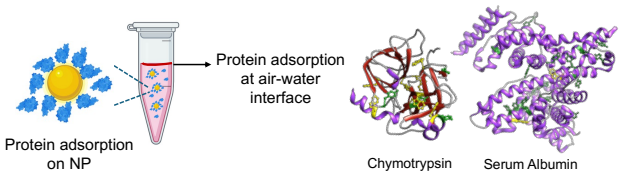
Protein adsorption
on NP
Protein adsorption
at air-water
interface
Chymotrypsin
Serum Albumin